Construction Engineering
Research Laboratory

**US Army Corps
of Engineers**®
Engineer Research and
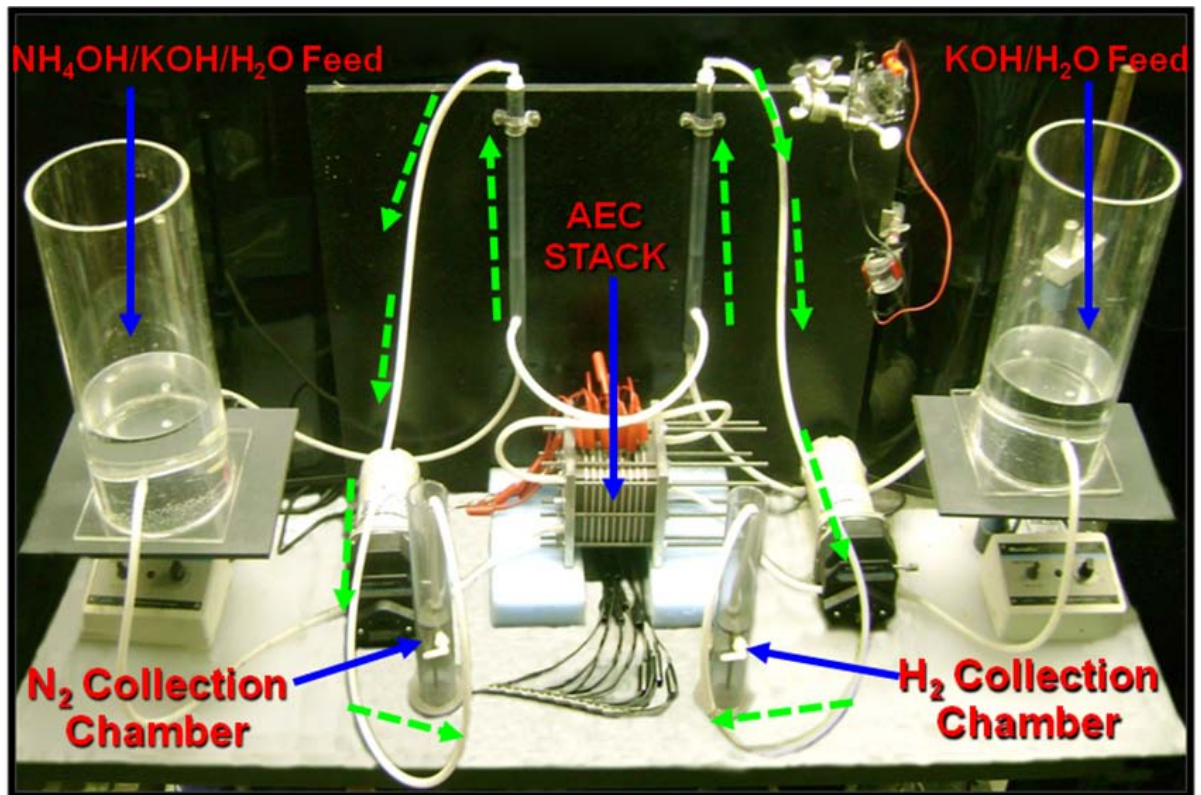Development Center

Electro Decomposition of Ammonia into Hydrogen for Fuel Cell Use

Gerardine G. Botte, and Carl A. Feickert

January 2012

Electro Decomposition of Ammonia into Hydrogen for Fuel Cell Use

Gerardine G. Botte
Center for Electrochemical Engineering Research
Ohio University
165 Stocker Center
Athens, OH 45701

Carl A. Feickert
Construction Engineering Research Laboratory (CERL)
U.S. Army Engineer Research and Development Center
2902 Newmark Dr.
Champaign, IL 61822-1076

Final Report

Abstract

This work was undertaken to create an efficient process for electrolyzing ammonia, by clarifying the electrolytic decomposition pathways of ammonia and urea. This project demonstrated the feasibility of using ammonia and urea electrolysis technologies to produce hydrogen as a potential fuel source for the fuel Proton Exchange Membrane (PEM) fuel cell back up power for training facilities and soldier camps, under the "Silent Camp" initiative. This was achieved with scaling of bench scale electrolyzer to a 50 W electrolyzer system known as the "GreenBox." The construction of the 50 W GreenBox depended on the development of the catalyst and fundamental understanding of the reaction mechanisms for ammonia and urea electrolysis. Significant progress in catalyst development was achieved by using chemical and electrochemical preparation techniques, and using the various state-of-the-art analytical methods funded through this project. A new synthesized material—nickel hydroxide nanosheets—has shown potential to be catalyst for urea electrolysis and catalyst support for ammonia electrolysis. The energy consumption for the ammonia electrolysis using the nickel based nanostructured electrodes is anticipated to be lower than 8.6 Wh per gram of hydrogen gas produced. The low energy consumption will provide a significant advantage when the GreenBox is combined with fuel cells.

Table of Contents

List of Figures and Tables

Figures

Tables

Preface

1 Introduction

1.1 Background

The standard method of power generation in military base camp operations is via the use of diesel generators. Unfortunately, diesel generators are often noisy and inefficient. Base camps could benefit from a "silent camp™" operation, in which power is supplied via low-noise, low-impact methods such as fuel cells. Fuel cells can run on a variety of fuels, but the commercially available Proton Exchange Membrane (PEM) fuel cell requires pure hydrogen, which can be commonly derived from the electrolysis of water.

Hydrogen can also be supplied by electrolyzing ammonia or urea, both of which are found in wastewater. Of the two, ammonia has a higher hydrogen fraction of atomic mass (17.65%) than water. Two technologies developed by Ohio University can process wastewater (ammonia and urea) into hydrogen, nitrogen, and clean water using renewable energy—the low energy consumption "ammonia and urea electrolyzers." These two technologies may find direct application for the production of hydrogen for distributed power. It is anticipated that the hydrogen produced by these novel processes may be used to run a fuel cell to generate electrical power, thus providing a safe and convenient alternative to diesel generators. The technologies also have the potential for non-military applications (e.g., agricultural wastewater, municipal wastewater, etc). The key feature of the ammonia and urea electrolysis processes is the low energy consumption for the production of hydrogen from ammonia and urea.

This work was undertaken to create an efficient and feasible process for electrolyzing ammonia, specifically, by clarifying the electrolytic decomposition pathways of ammonia (NH_3) and urea ($CO(NH_2)_2$). These chemicals are typically found in the excretions of all higher order vertebrates, and can be readily found in feedlot run-off, municipal sanitary systems, etc. The pathways for the electro-decomposition of these chemicals are reasonably well understood. For example, several mechanisms had been proposed in the literature for the oxidation of ammonia in alkaline media (Oswin and Salomon 1963, Gerischer and Mauerer 1970, de Vooys et al. 2001), however, the final mechanisms have not been reported. Further-

more, most of the mechanisms proposed in the literature do not account for the adsorption of OH⁻ ions on the catalyst, which has been reported to affect the oxidation of ammonia (Botte 2004, Cooper and Botte 2006).

Also, it is important to know how to catalytically execute these processes, using energetically efficient and mechanically robust electrodes employing highly specific materials formulation coupled with innovative geometries. There exist a large number of potential catalytic compositions and design geometries. Further, the details of the evolved gases depend on the electrode's material and surface geometry parameters. A detailed correlation between the evolved gases and these material parameters is required for efficient use of this chemical decomposition process.

1.2 Objectives

The specific objectives of the Phase I of this project were to:

1. Determine kinetics and operating parameters required for the scale up of the ammonia and urea electrolyzers.
2. Evaluate and optimize the performance of bench-scale prototypes (50 W) with synthetic wastewater.
3. Provide the required information for a scale-up prototype (500 W).

1.3 Approach

The objectives of Phase I of the project were accomplished through the following tasks:

*   Ammonia and urea electrolysis methods were compared with existing water electrolysis technology. Improvements in ammonia and urea electrolysis technologies and advancements in the catalyst development were noted (Chapter 2).
*   A 50 W GreenBox system, which was a scaled up version of the bench scale single cell ammonia and urea electrolysis system, was built and tested, in anticipation of the assembly of a 500 W electrolyzer in the Phase II of the project (Chapter 3).
*   Reaction mechanisms for the electrochemical oxidation of ammonia and urea were investigated considering both modeling and experimental work for a rational design of the catalyst, and using molecular modeling and prior experimental studies to advance reaction mechanisms of ammonia and urea electrolysis (Chapter 4).

- Catalysts with higher catalytic activity for efficient electrolysis were developed (Chapter 5).
- The potential for application of the ammonia and urea electrolysis technologies in DoD programs and civilian applications were explored with special emphasis on wastewater remediation (Chapter 6).

1.4   Mode of technology transfer

This report will be made accessible through the World Wide Web (WWW) at URL: http://www.cecer.army.mil

2 Efficiency of Ammonia and Urea Electrolysis

2.1 Ammonia electrolysis

Ammonia, which is found in wastewater, has a higher hydrogen fraction of atomic mass (17.65%) than the water molecule. The electrolysis of ammonia in an alkaline medium results in the formation of hydrogen gas at the cathode electrode and nitrogen gas at the anode electrode. In this process, the electrocatalyst used for the oxidation reaction of ammonia is platinum-iridium (Pt-Ir) alloy, which is supported on a substrate (e.g., carbon fiber, metal, carbon paper, etc). The electrochemical reactions for the ammonia electrolysis process are:

Anodic reaction

$$2\,NH_3 + 6\,OH^- \rightarrow N_2 + 6\,H_2O + 2\,e^- \quad E° = \text{-0.77 V vs. SHE}$$

Reaction 1

Cathodic reaction

$$2\,H_2O + 2\,e^- \rightarrow H_2 + 2\,OH^- \quad E° = \text{-0.829 V vs. SHE}$$

Reaction 2

Overall reaction

$$2\,NH_3 \rightarrow N_2 + 3\,H_2 \quad E° = 0.059\,V$$
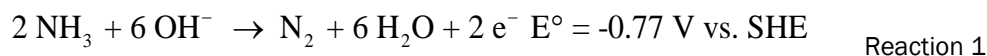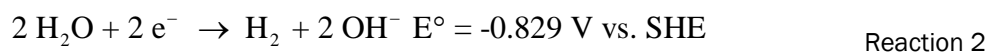
Reaction 3
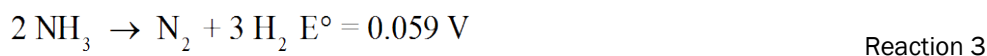
Thermodynamically, the electrochemical splitting of ammonia into hydrogen (H_2) and nitrogen (N_2) requires only 59 mV, whereas the thermodynamic cell voltage for water electrolysis is 1.23 V. Theoretically, the electrolysis of ammonia should consume 1.55 Wh to produce 1 g of hydrogen gas. However, the energy consumption for different ammonia electrolysis systems varies with different catalysts, support materials, and electrolytic cell configurations. Table 1 lists the characteristics of three such systems, along with the advantages and drawbacks found in each system.

Table 1. Energy consumption for hydrogen production in different ammonia electrolysis systems.

System	Cell Voltage (V)	Energy Consumption (Wh/g of H_2)	Comments
1 Pt-Rh catalyst on carbon fiber (Single cell)	0.33 (5 M NH_3 and 50 °C)	8.6	• Each experiment was performed in a closed cell with the circulating electrolyte. • All the electrodes are electrically connected with Ti wire, which is not a good electrically conducting material. • The Pt-Rh catalyst is not the best catalyst for the electrolysis of ammonia. Catalyst performance can be improved by adding Ir. *Recommendations:* • Need better cell design for NH_3 electrolysis. • Use electrically conducting material such as Ni instead of Ti. • Use Pt-Ir catalyst for ammonia electrolysis.
	0.39 (5 M NH_3 and 25 °C)	10.0	
	0.5 (0.5 M NH_3 and 50 °C)	12.2	
	0.65 (0.5 M NH_3 and 25 °C)	15.5	
2 Pt-Ir catalyst on carbon fiber paper (~15.5 mg/cm^2) (Biradar 2007)	0.36 (1 M NH_3, single open cell and 55 °C)	9.6	• The electrodes have high loading of Pt-Ir over carbon fiber paper. • The catalyst support material – carbon fiber paper is brittle. • Ti frame and wires from the electrodes were used for electrical contact. *Recommendations:* • Reduce the Pt-Ir catalyst loading. • Change the carbon paper to a mechanically stronger and electrically good conductor support material. • Modify the cell design to improve easy flow of electrolyte and gas removal without creating a significant back pressure.
	0.46 (1 M NH_3, single open cell and 25 °C)	12.3	
	0.56 (1 M NH_3, 9-cell stack and 55 °C)	15.4	
	0.63 (1 M NH_3, 9-cell stack and 25 °C)	17.3	
3 Pt-Ir catalyst on carbon fiber paper (12.4 mg/cm^2) (Boggs and Botte 2009)	0.52 (5 M NH_3 solution, closed cell and room temperature)	15	

2.2   Recommendations regarding ammonia electrolysis

Of the three systems described, System 1 offers the most promising opportunity to extend the catalyst composition by using a better electronically conductive tab for the electrode. Phase II of this project will continue to focus on adapting the electroplating capabilities of System 1, which consumes the least energy in the production of hydrogen, through the use of more highly electronically conductive tabs (e.g., nickel tabs).

The experimental data from a 9-cell stack electrolyzer for ammonia (Figure 1), was used to illustrate the energy consumption required to produce 1 g of hydrogen gas. The electrodes in this electrochemical cell had a high loading of Pt-Ir over carbon fiber paper (System 2 in Table 1). The ammonia electrolysis in the 9-cell stack electrolyzer was operated at 4.5 amps, which resulted in a cell voltage of 0.63 V at 25 °C and produced 0.164 g of hydrogen per hour (System 2 in Table 1). In other words, the 9-cell stack ammonia electrolyzer required 17.3 Wh of electrical energy to produce 1 g of H_2.

Unfortunately, the system showed a significant ohmic overpotential due to: (1) the use of titanium tabs, (2) electrical losses through the connecting wires, and (3) high electrical resistance in the contact between the wires and the tabs. To overcome this, Phase II of this project will need to include a significant study of ohmic overpotential minimization through the tabs and electrical connections through the construction of the 500 W urea electrolyzer.

By comparison, water electrolysis consumes more energy than does ammonia electrolysis to produce the same amount of hydrogen gas. The National Research Council and National Academy of Engineers report on the "hydrogen economy" (NRC & NAE 2004) states that a commercial water electrolyzer requires 1050 kW of power to produce 8290 scf of H_2 (21103.7 g of H_2) per hour, or 49.75 Wh/g. An ammonia electrolyzer, which uses 17.3 Wh to produce the same result, is 65.1% more efficient than a commercial water electrolyzer.
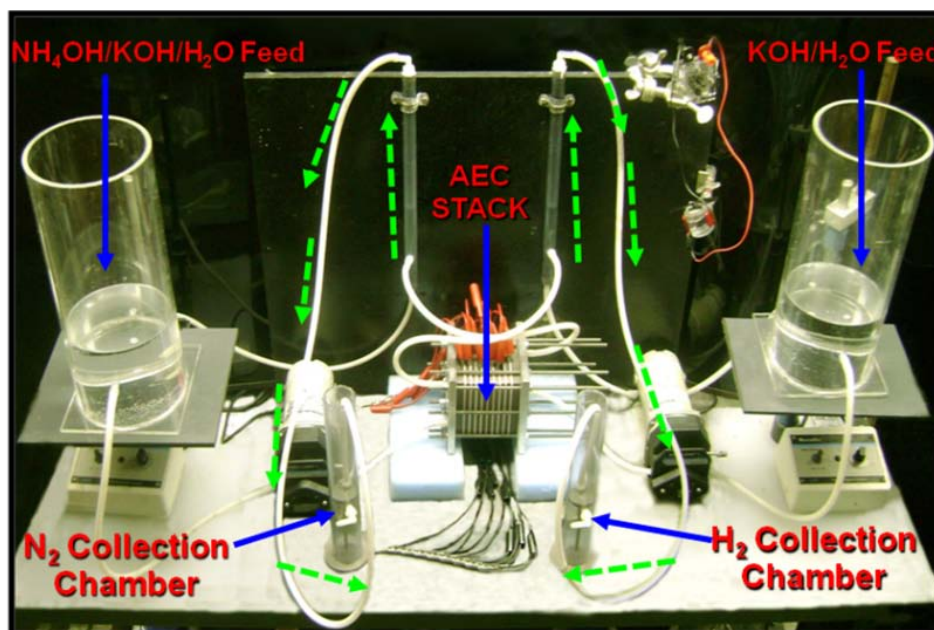
Figure 1. Experimental set up of the 9-cell stack of the ammonia electrolytic cell (AEC). During ammonia electrolysis, the collection chambers at the cathode and anode side accumulated the hydrogen and nitrogen gases, respectively.

2.3 Urea electrolysis

Urea is used as fertilizer and is also found in the liquid waste of human and other animals. The electrochemical oxidation of urea can remediate wastewater and also produce hydrogen gas, a high-value product. The active catalyst for electrochemical oxidation of urea is nickel. (In contrast, the active catalyst for ammonia electrolysis is platinum.) The electrochemical reactions for the urea electrolysis are:

Anodic reaction

$$CO(NH_2)_2 + 6\,OH^- \rightarrow N_2 + 5\,H_2O + CO_2 + 6\,e^- \quad E° = \text{-0.46 V vs. SHE} \qquad \text{Reaction 4}$$

Cathodic reaction

$$6\,H_2O + 6\,e^- \rightarrow 3\,H_2 + 6\,OH^- \quad E° = \text{-0.829 V vs. SHE} \qquad \text{Reaction 5}$$

Overall reaction

$$CO(NH_2)_2 + H_2O \rightarrow N_2 + 3\,H_2 + CO_2 \quad E° = 0.369\ V \qquad \text{Reaction 6}$$
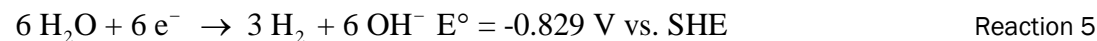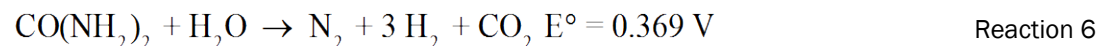
The electrochemical oxidation of urea thermodynamically requires only 0.369 V and produces hydrogen, nitrogen, and carbon dioxide gases. (By contrast, water electrolysis requires 1.23 V.) Table 2 lists two electrolytic cells with different kinds of catalyst and electrode configuration for the production of hydrogen gas.

2.4   Recommendations for Phase II (urea electrolysis)

Overall, development of the Ni-Rh catalyst (Case 2), with improvement on preferentially depositing Rh(111) over the Ni electrodes, will be performed in Phase II of this project. Nano-sized Ni-Rh electrode could increase the current density for the urea electrolysis. There are also promising signs from the other catalysts, Ni-Co hydroxide (Case 3) and $Ni(OH)_2$ nanosheets (Case 4). Phase II will perform more systematic investigations to develop nano-sized catalysts along the lines of $Ni(OH)_2$ nanosheets.

The single urea electrolytic cell with Ni-Rh electrodes (Case 2 listed in Table 2), of which the lower half of the Ni electrode is covered with Rh, was subjected to 1.6 V, and the urea solution (0.33 M urea + 5 M KOH) was circulated once through the anode side. This electrolytic cell generated hydrogen gas at a rate of 0.001 g/minute with an average current of 1.311 A. This single cell consumed 34.96 Wh to produce 1 g of hydrogen, at least 29.7% less energy than water electrolyzer, which consumed 49.75 Wh to produce 1 g of hydrogen.

Table 2. Energy consumption for hydrogen production in different urea electrolysis systems

Systems	Cell Voltage (V)	Energy consumption (Wh/g of H_2)	Comments
1. Nickel oxyhydroxide (NiOOH) modified Ni electrode (2.5 mg/cm^2) (Boggs, King, and Botte 2009)	1.4	37.5	• A 2 cm x 2 cm size electrode was studied. • Ni sheet was the catalyst support material and electrical contact of the electrode. *Recommendations:* • Increase the surface area of the catalyst and the support material. • Use bimetallic or Ni based alloy catalyst to overcome surface blockage due to CO.
2. Rh deposited Ni mesh electrode (0.5 mg/cm^2 of Rh covering lower half of Ni mesh electrode)	1.6	34.96	• Room temperature operation. • Single pass on the anode side of the electrolytic cell. • Various parameters of the electrolysis process were not optimized. • The particle size was larger and the crystal plane of Rh was not well defined. *Recommendation:* • Develop nano-sized Ni-Rh catalyst and deposit preferentially Rh(111). • All the operating parameters for the urea electrolyzer have to be optimized.
3. Ni-Co hydroxide		Promising performance to be measured in Phase II	• Bench scale experiments with small electrodes. • Gas collection and its analysis have to be performed. *Recommendations:* • Systematic experimentation to collect and measure the anode and cathode gases. • Scale up of the 43% (at.wt.) Co added Ni(OH)$_2$ catalyst for GreenBox application.
4. Ni(OH)$_2$ nanosheet		Promising performance to be measured in Phase II	• Nanosized catalyst for urea electrolysis. • Uses Teflon binding material to attach the nanosheets to an electrically conducting substrate • Very high surface area available for the electrocatalytic activity *Recommendations:* • Investigate on adherence of the nanosheet to the conducting material without Teflon binder. • Plating of other catalyst over the nanosheets so as to use nanosheets as support material. • Scale up of the nanosheets to the GreenBox size electrodes.

3 Test of 50 W GreenBox

Part of the effort in Phase I of the project focused on the demonstration of the scale up of the urea electrolysis process from a single cell bench scale into a urea electrolyzer stack. Knowledge obtained from the scale up process was used in the design of the 500 watts electrolyzer, which is part of Phase II of the project.

3.1 Cell design

In the electrochemical oxidation of urea, nickel is the active material. (More specifically, Ni^{2+}/Ni^{3+} redox couple is the required electrocatalyst.) During the urea electrolysis, carbon-based compounds or intermediates were formed on the electrode surface, which have been observed to block or interfere with the nickel active sites. To address this problem, rhodium (Rh) was deposited on the Ni electrodes to help in preventing the build up or surface blockage of Ni sites by carbon-based compounds, which could in turn maintain or enhance the reaction rate for electrochemical oxidation of urea.

Figure 2 shows the initial design for a large size single cell to perform urea electrolysis. The cell has end plates to hold the electrode and a membrane is used to separate the anode side from the cathode side. The membrane is held in place by two gaskets. This cell has a provision to fill the electrolyte on each side of the electrode by using the inlet and outlet provided at the top and bottom of each end plate. The single cell can perform the urea electrolysis experiment under static or flow conditions.

This design of the single cell is for planar electrodes, where both anode and cathode electrodes are nickel (Ni) sheets, but where each has different amounts of rhodium (Rh) loadings. The electrode dimension was 7 x 7-in. and Rh was deposited only in the lower half of the electrode. The anode electrode had Rh loading of 0.5 mg/cm² and the cathode electrode was loaded with 1 mg/cm² of Rh. After an hour of testing the single cell shown in Figure 2, the oxidation current for urea at 1.6 V was only 1.16 A. This translates to urea oxidation current density of only 3.7 mA/cm². To improve the electro-oxidation current for urea, the electrode design was modified to an extended oval shape (Figure 3).
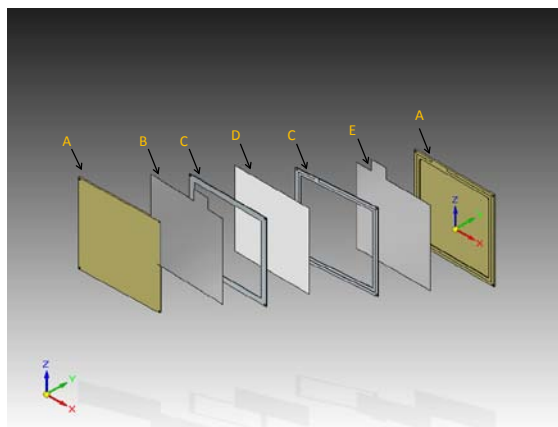
Figure 2. Exploded view of the first large scale single cell designed to perform urea electrolysis. The cell comprises of end plate (A), anode electrode (B), gasket sheet (C), membrane (D), and cathode electrode (E).
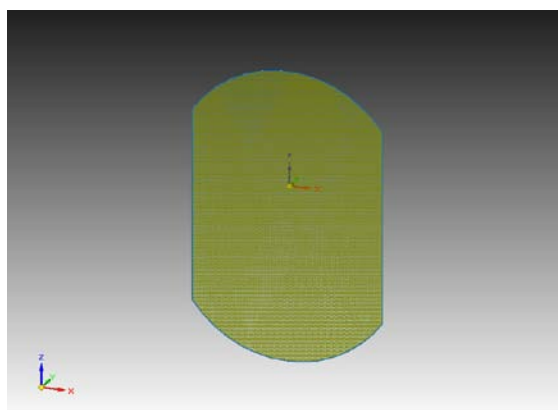
Figure 3. Diagram of the new electrode for urea electrolysis. This electrode (Ni mesh #40) is the base material for both anode and cathode electrodes of the GreenBox.

Measured between its top and bottom hemisphere, the new Ni mesh electrode is 6-in. wide and 9-in. long. The Rh catalyst was deposited on the lower half of the Ni mesh electrode with 0.5 mg/cm^2 loading for the anode electrode and 1 mg/cm^2 loading on the cathode electrode. A single cell was developed using this new electrode design. Figure 4 shows an exploded view of the design. The membrane used to separate the anode and the cathode side of the single cell is held in place by a O-ring located in the end plate. This O-ring also provides a good seal for liquid and gases. There were no leaks observed from the single cell during urea electrolysis. The advantage in using the new Ni mesh electrodes is the design of the electrode. The extended oval shape of the electrode along with wire mesh provides larger surface area than the rectangular electrode shown in Figure 2. The extended oval shape of the electrode is also grooved in the inner side of the end plate (Figure 4), which facilitates easy removal of gas bubbles from the cell and prevents a build-up of back pressure inside the electrolytic cell.
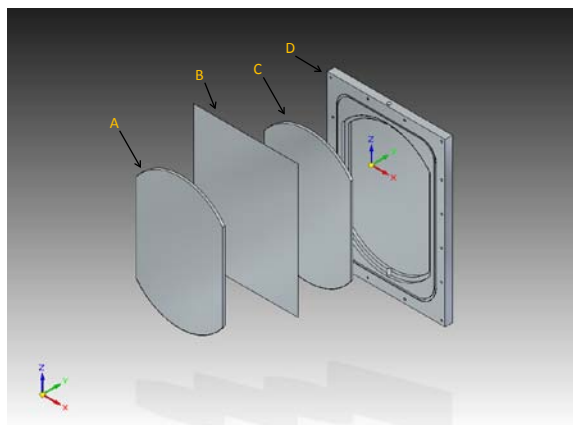
Figure 4. Sectional exploded view of the single cell assembled based on the new electrode design. The anode electrode (A) and the cathode electrode (C) are separated by a membrane (B). The electrodes are covered to the external atmosphere by an end plate (D).

3.2 Single cell testing

The extended oval shaped Ni mesh electrodes with Rh loading were assembled in the new single cell. Each single cell was tested for urea electrolysis under a condition of flow. The electrolyte used in both the anode and the cathode sides was 0.33 M urea + 5 M KOH. The urea concentration chosen in the electrolyte for the experiments reflects the average amount of urea observed in human urine, 20 g/L/day. Figure 5 shows the flow diagram of a single cell testing setup. Testing was done to evaluate a few parameters on the production of hydrogen gas, and to evaluate the percentage of urea conversion. The urea conversion rate was determined for the single cell system where the anode electrolyte flowed through the urea electrolytic cell once (in a single pass).
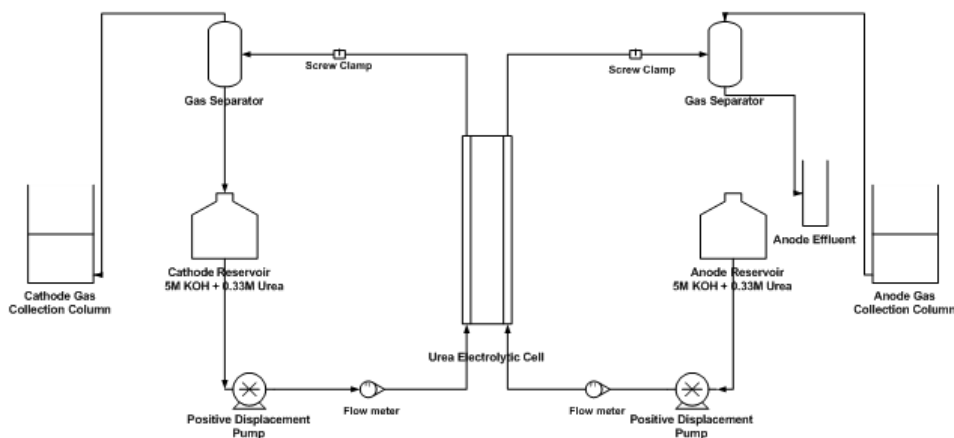
Figure 5. Flow diagram of the single cell testing set up. The cathode electrolyte is circulated through the cathode side of the cell whereas the anode electrolyte is passed through the anode side only once (single pass) to evaluate the urea conversion percentage.

As Figure 5 shows, the cathode solution is pumped into the cathode side of the single cell from its reservoir. The spent cathode solution from the urea electrolytic cell passes through a gas separating column, where the hydrogen gas is separated from the urea solution, and from where the solution flows back into the cathode reservoir. The separated hydrogen gas is collected in a gas column using the water displacement principle. Similar to the cathode side, the anode solution is pumped into the anode side of the urea electrolytic cell from its reservoir. The spent anode solution also goes through a gas separating column. Since these experiments used a single pass for the anode solution, the anode effluent was collected for urea analysis. The separated anode gases were also collected in a gas collecting column. The volume of gases collected in the anode and cathode sides was measured over the testing duration.

The single cell test with single pass on the anode side evaluated these parameters: cell voltage, anode electrolyte flow rate, and cathode electrolyte flow rate (Table 3). Note that Minitab® software* was used to prepare the Box-Benkhen surface response experimental design and also to statistically analyze the results.

Table 4 lists the results of 15 single cell tests. Note that the anode flow rate in Tables 3 and 4 represent readings of the pump settings, and not the measured flow rate of the electrolyte. The exact flow rate corresponding to the pump settings was found separately, and the anode electrolyte flow rate relating the reading values was used in the statistical analysis. The urea concentration in the anode effluent was determined using the spectrophotometric method. The urea conversion percentage was calculated from the ratio of the urea concentration in the anode effluent to the anode solution.

The data in Table 4 show that Experiment No. 5 shows zero hydrogen gas produced, at 1.4 V with the cathode electrolyte flow rate of 75 mL/min and anode flow reading of 5, is an anomalous value. The amount of hydrogen gas collected in the column during that experiment was very minimal and the volume of the hydrogen gas in the column was not sufficient enough to measure.

---

* Minitab® Software for Quality Improvement, http://www.minitab.com

Table 3. Parameters and its levels used for the single cell testing.

Parameter	Low	Medium	High
Potential (V)	1.4	1.5	1.6
Anode Flow Reading	5	18.75	32.5
Cathode Flow Rate (mL/min)	30	75	120

Table 4. Experimental results from the single cell testing with hydrogen production rate and urea conversion percentage.

Run Order	Std Order	Pt Type	Blocks	Anode Flow	Cathode Flow (mL/min)	Potential (V)	Hydrogen (g/min)	Urea Conversion (%)
1	1	2	1	5	30	1.5	0.0002	23.51
2	9	2	1	18.75	30	1.4	0.00002	29.73
3	10	2	1	18.75	120	1.4	0.0003	25.83
4	7	2	1	5	75	1.6	0.0007	25.83
5	5	2	1	5	75	1.4	0	26.12
6	13	0	1	18.75	75	1.5	0.0003	22.08
7	14	0	1	18.75	75	1.5	0.0002	2.21
8	2	2	1	32.5	30	1.5	0.0002	24.55
9	8	2	1	32.5	75	1.6	0.0009	23.89
10	12	2	1	18.75	120	1.6	0.001	18.68
11	6	2	1	32.5	75	1.4	0.00002	3.64
12	11	2	1	18.75	30	1.6	0.0007	2.77
13	3	2	1	5	120	1.5	0.0002	20.44
14	15	0	1	18.75	75	1.5	0.0003	24.39
15	4	2	1	32.5	120	1.5	0.0002	11.29

A surface response analysis of the results listed in Table 4 was done to determine the optimum conditions to maximize hydrogen production (Figure 6). Figure 6 shows that if the anode electrolyte flows at a rate of 7.8 mL/min with cathode solution flowing at 120 mL/min and at a cell voltage of 1.6 V, the single cell should be able to produce the largest volume of hydrogen gas.

The urea conversion from the single pass urea electrolysis in a single cell was also studied using the surface analysis and the optimization plot for maximizing urea conversion (Figure 7). The maximum percentage of urea can be converted into its gases when the anode electrolyte flow rate is maintained at 1.1 mL/min with the cathode solution flowing at 120 mL/min and with a cell voltage of 1.6 V applied to the single cell.
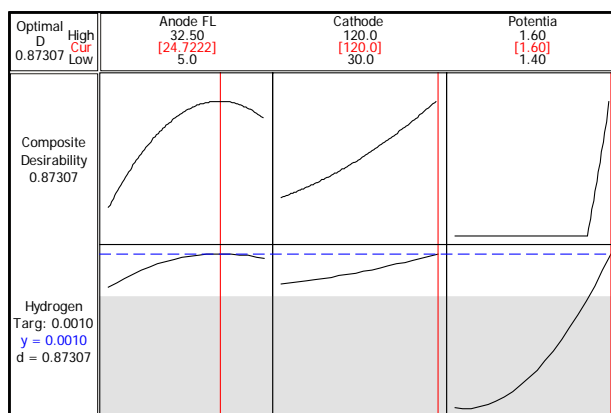
Figure 6. Optimization plot for hydrogen production in a single pass testing of the single urea electrolytic cell. Optimum values for obtaining maximum hydrogen production are anode flow rate 7.8 mL/min, cathode flow rate 120 mL/min, and cell voltage 1.6 V.
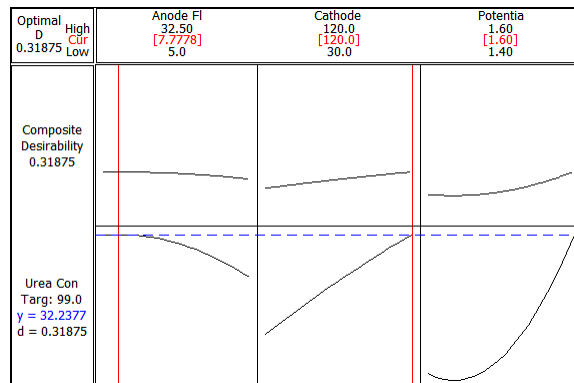
Figure 7. Optimization plot for urea conversion from single pass testing in a single urea electrolytic cell. The optimum conditions for obtaining maximum urea conversion are anode flow rate 1.1 mL/min, cathode flow rate 120 mL/min, and cell voltage 1.6 V.

The optimum value for the anode flow rate changes if both hydrogen generation rate and urea conversion percentage are considered in combination. Figure 8 shows the optimization plot for the combination of the hydrogen production and urea conversions, in which the anode flow rate is increased to 17.9 mL/min with other two parameters are maintained at the same value (of 120 mL/min for cathode flow rate and 1.6 V for cell voltage).

3.3   50 W GreenBox testing

The GreenBox system was designed to remove urea from wastewater and produce hydrogen gas. Each urea electrolytic cell as shown in Figure 4 was assembled together into a stack of 10 cells to form the first prototype GreenBox system (Figure 9). The GreenBox is expected to consume 50 W of electrical energy.
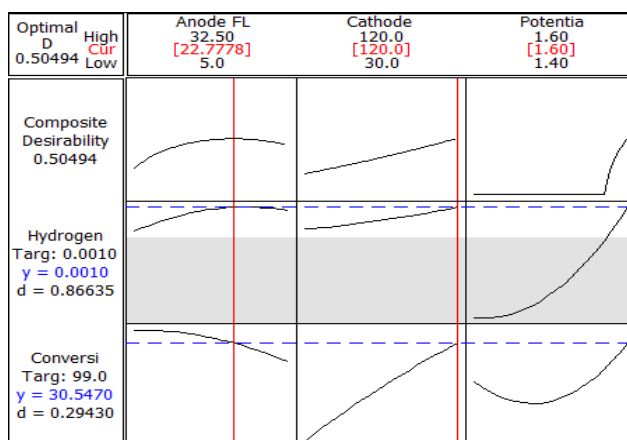
Figure 8. Optimization plot for the combination of hydrogen production and urea conversion using single pass testing in a single urea electrolytic cell. The optimum values are anode flow rate 17.9 mL/min, cathode flow rate 120 mL/min, and cell voltage 1.6 V.
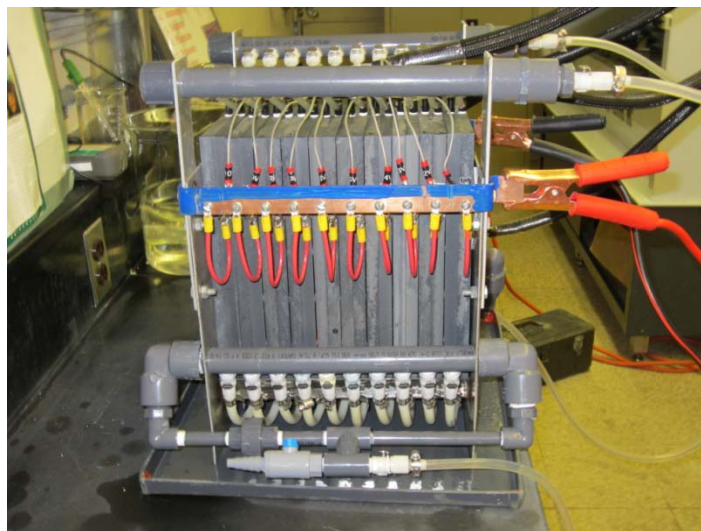
Figure 9. Photo of the GreenBox, which has 10 cells stacked together. The electrolyte inlets to the anode and cathode sides are at the bottom and the outlets for the solutions are placed on the top.

Testing of the GreenBox required a well controlled and monitored test stand so a test stand was built at the Center for Electrochemical Engineering Research (CEER) to regulate electrolyte flow into each cell, and to monitor pressure, temperature, pH, and gas flow rate. Figure 10 shows a flow diagram of the electrolyzer test stand connected to the GreenBox. The liquid/gas separator for the cathode and anode side is used as the reservoir for the corresponding electrolyte. The cathodic side pump draws the electrolyte from the cathode liquid/gas separator and pumps the solution into the cathode side of the GreenBox system via a manifold. The flow rate of the electrolyte in the cathode side is maintained and regulated by the liquid flow meter (LFM) and the flow control valve (FC).
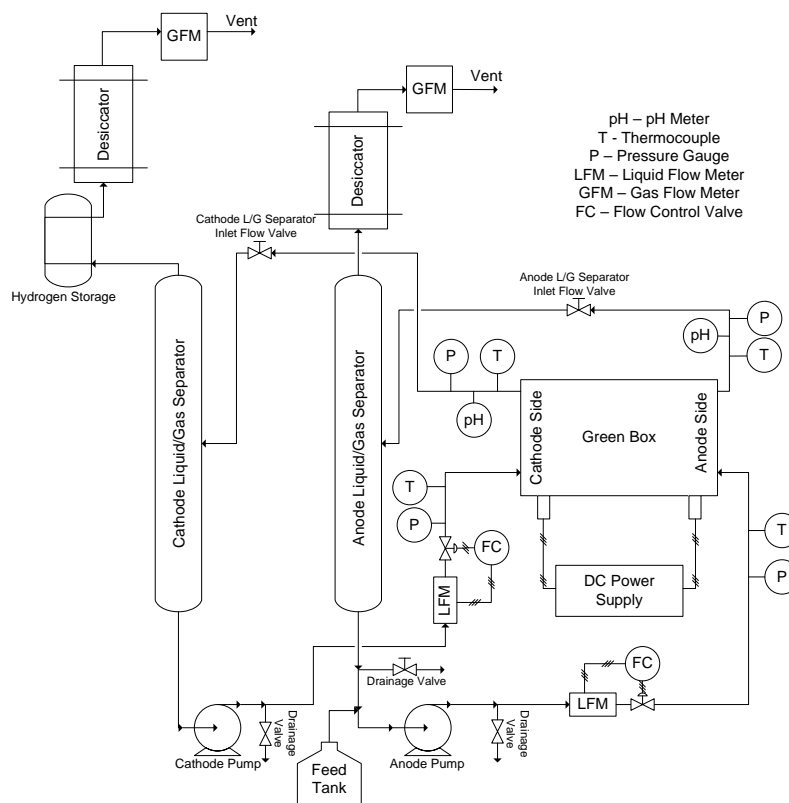
Figure 10. Flow diagram of the home built electrolyzer test stand. The electrolyzer test stand is connected to the GreenBox system.

The inlet and outlet temperature and pressure of the cathode electrolyte are monitored. The pH of the cathode electrolyte is monitored on the outlet side. The cathode electrolyte exiting the GreenBox system carries hydrogen gas, which is separated in the liquid/gas separator. The hydrogen gas is collected in a water column (labeled as hydrogen storage in the flow diagram). Before venting, the hydrogen gas passes through a desiccator to remove moisture and then through a gas flow meter.

The test stand components on the anode side of the electrolyzer are similar to those on the cathode side described above. An additional feature included in the anode side is a drainage valve at the tube line coming from the end of anode liquid/gas separator so that the anode effluent from the anode side of the GreenBox can be drained out during single pass experiments for testing and monitoring. In the single pass experiments, the anode pump draws the electrolyte from a feed tank. The GreenBox is supplied with cell voltage by a DC power supply unit. The controls on the flow meter, thermocouple, pressure transducers, and pumps are digitally regulated through data acquisition unit, which is in turn observed by a program developed in Camille software. The program is capable of digitally controlling, monitoring, and

recording the parameters mentioned above along with cell voltage and current for all the 10 cells. Figure 11 shows a screenshot of the program developed to record and control the parameters.

Preliminary experiments using the GreenBox were performed with the help of the electrolyzer test stand. These experiments used potassium hydroxide solutions of different concentrations to generate a baseline values before using urea solutions in the GreenBox. In all the experiments, the electrolyte solution was constantly circulated with an anode flow rate of 80 mL/min and a cathode flow rate was maintained at 1200 mL/min. These flow rate values reflect the optimum flow rate values determined from the single cell testing for maximizing hydrogen gas production. The electrolyte concentrations used in the preliminary experiments until now were 0.01, 0.1, and 1 M KOH, which corresponds to pH value of 12, 13, and 14. The cell voltage for all the 10 cells was varied between 1.5 and 1.575 V for these experiments. Figure 12 shows the current-time response for the GreenBox over the period of entire experiment (3 hrs).

The individual cell was designed to have a maximum current of 3.2 A at 5 M KOH concentration. The current observed during the baseline experiments is low because it is mainly due to side reactions associated with the phase transition of the anode and parasitic losses.

The electrolysis of different concentrations of KOH solution in the GreenBox produces the hydrogen gas and the flow rate of the hydrogen gas over the 3-hr experiment (Figure 13). The hydrogen gas seen on the cathode side could be due to the slight water oxidation at these cell voltages for the different concentrations of KOH solution. It is hypothesized that the minor hydrogen gas produced is mainly due to the oxidation of nickel to its active form (Boggs, King, and Botte 2009), and not to a continuous process such as urea or water electrolysis.

The data in Figure 13 indicate that the production of hydrogen gas was higher at cell voltage of 1.575 V than at 1.5 V for pH 12 and 13 solutions, which was expected. Table 5 lists the average hydrogen flow rate at different KOH solutions and cell voltages. At cell voltage of 1.575 V, the average flow rate for the production of hydrogen increased more than 10 mL/min with one pH unit increase in the KOH solution. However, the hydrogen production rate was similar for KOH solutions of pH 13 and 14 at a cell voltage of 1.5 V.
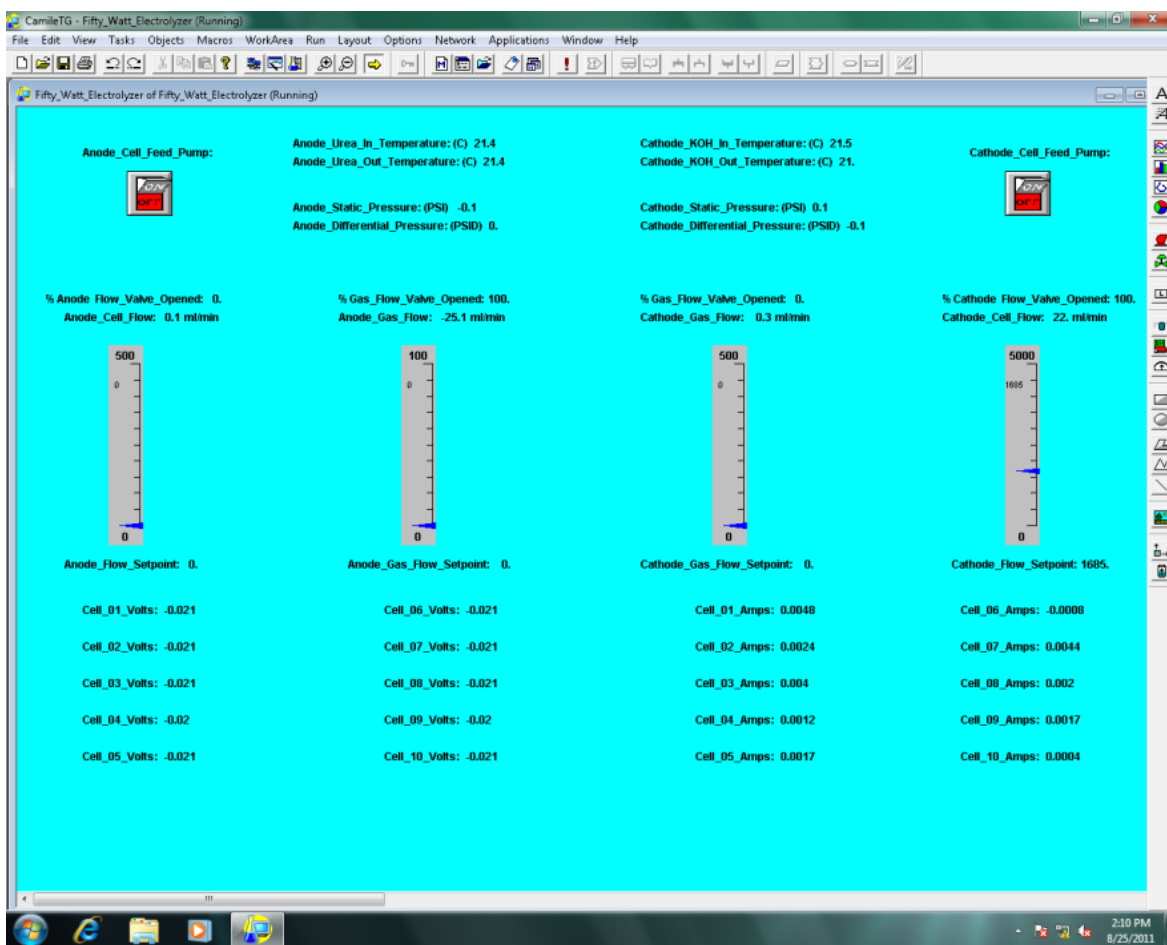
Figure 11. Screenshot of the data collection program developed using the Camille software. The program can record and control various parameters during electrolysis experiment using the electrolyzer test stand.
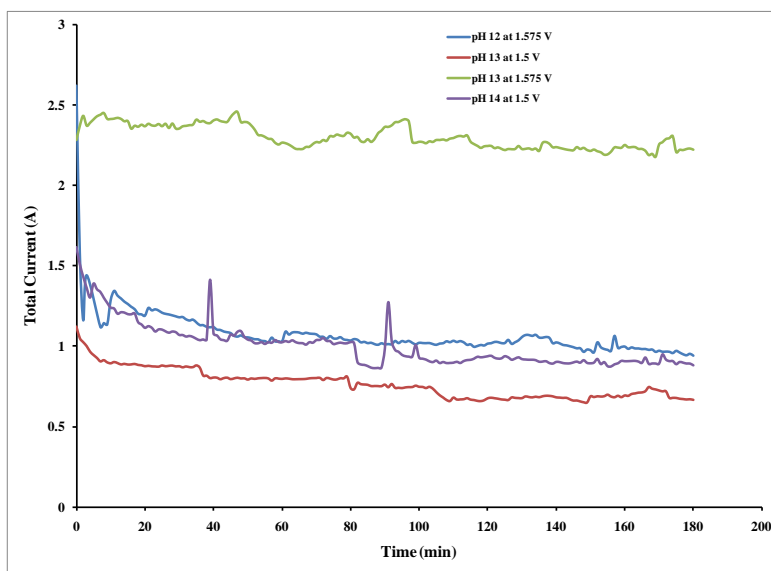
Figure 12. Current-time response of the GreenBox during electrolysis with potassium hydroxide solution. The electrolyte used in the experiment are 0.01 M KOH (pH 12), 0.1 M KOH (pH 13), and 1 M KOH (pH 14).
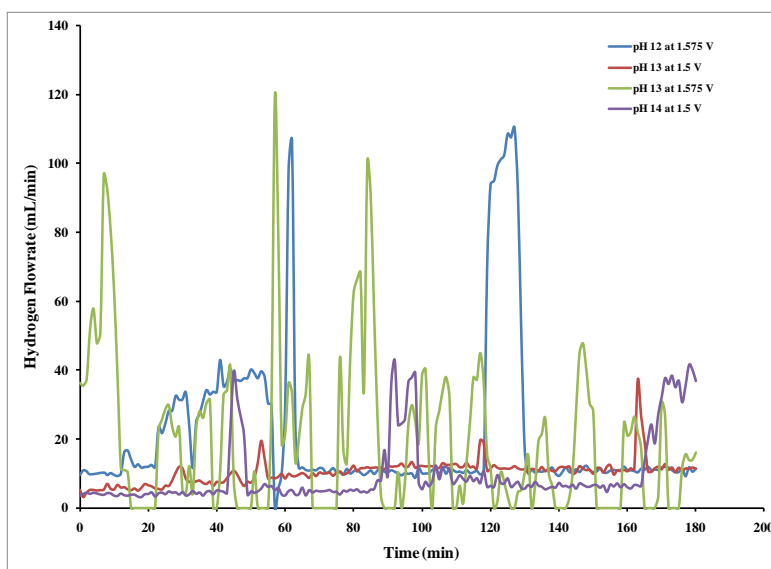
Figure 13. Plot of the hydrogen gas flow rate during the experimental time for various concentrations of KOH solution in the GreenBox.

Table 5. Hydrogen flow rate from water electrolysis in the GreenBox.

Electrolyte solution pH	Average hydrogen flow rate (mL/min)	
	1.5 V	1.575 V
12	–	16.32
13	10.44	27.88
14	9.81	–

No further experiments were conducted with the custom-built test stand on the 50 W GreenBox because of the many engineering problems and issues that developed while running the baseline experiments (i.e., proper functioning of the pumps, flow meters, and gas separation columns). The test stand is presently being redesigned to ensure that the working of each component is accurately assessed and calibrated. These issues have extended the evaluation and optimization of the 50 W GreenBox into Phase II of this project.

3.4   Recommendations for Phase II (GreenBox)

It is recommended that Phase II of this project include:

- further experiments with the GreenBox, which include urea solution containing 0.33 M urea
- further experiments that consider other parameters related to the urea electrolysis in the GreenBox system.

4 The Reaction Mechanisms

4.1 Electro-oxidation of ammonia

Two different reaction mechanisms for the electrochemical oxidation of ammonia in alkaline media have been proposed, one by Oswin and Salomon (1963), and one by Gerischer and Mauerer (1970). The reaction steps proposed by Oswin and Salomon, in 1963, for the oxidation of ammonia are:

$$NH_3 + M \ \square \quad MNH_3 \qquad \qquad \text{Reaction 7}$$

$$MNH_3 + OH^- \ \square \quad MNH_2 + H_2O + e^- \qquad \text{Reaction 8}$$

$$MNH_2 + OH^- \ \square \quad MNH + H_2O + e^- \qquad \text{Reaction 9}$$

$$MNH + OH^- \ \square \quad MN + H_2O + e^- \qquad \text{Reaction 10}$$

$$MN + MN \ \square \quad M_2N_2 \qquad \qquad \text{Reaction 11}$$

$$M_2N_2 \ \square \quad N_2 + 2\,M \qquad \qquad \text{Reaction 12}$$
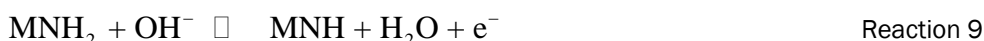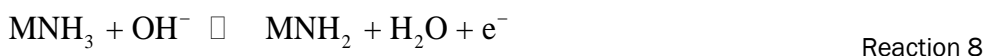
where:

M represents the catalyst material
The electrochemical reactions takes place on the catalyst surface.

Gerischer and Mauerer (1970) proposed a reaction mechanism for the ammonia electro-oxidation with inclusion of extra reaction steps to the ones suggested by Oswin and Salomon:

$$NH_3 + M \ \square \quad MNH_3 \qquad \qquad \text{Reaction 7}$$

$$MNH_3 + OH^- \ \square \quad MNH_2 + H_2O + e^- \qquad \text{Reaction 8}$$

$$MNH_2 + OH^- \ \square \quad MNH + H_2O + e^- \qquad \text{Reaction 9}$$

$$MNH + OH^- \ \square \quad MN + H_2O + e^- \qquad \text{Reaction 10}$$

$$MN + MN \ \square \quad M_2N_2 \qquad \qquad \text{Reaction 11}$$

$$MNH_x + MNH_y \ \square \quad M_2N_2H_{(x+y)} \qquad \text{Reaction 13}$$

$$M_2N_2H_{(x+y)} + (x+y)\,OH^- \ \square \quad M_2N_2 + (x+y)\,H_2O + (x+y)\,e^- \qquad \text{Reaction 14}$$

$$M_2N_2 \ \square \quad N_2 + 2\,M \qquad \qquad \text{Reaction 12}$$
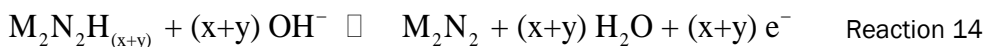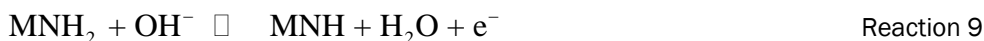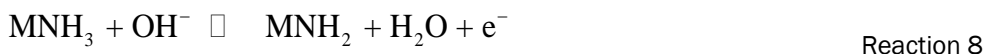
The steps in the Gerischer and Mauerer reaction mechanism follow the same reactions listed by Oswin and Salomon except for those shown in Reactions 13 and 14 . According to Gerischer and Mauerer, additional reactions and intermediates are formed during the electrochemical oxidation

of ammonia. The secondary reactions involves other intermediates such as NH_x and NH_y (x and y = 1 or 2). These NH_x and NH_y intermediate molecules can combine to form N_2H_2, N_2H_3, and N_2H_4 molecules (Reaction 13), which eventually react with OH^- ions to form adsorbed N_2 and water molecules (Reaction 14).

The development of a highly efficient electrocatalyst for the oxidation of ammonia requires a thorough understanding of different reaction steps involved in the mechanism. Molecular modeling of the reactions steps provides information on the structural changes of each molecule with the catalyst surface. Additionally, the reaction rates of the different reaction steps mentioned in both mechanisms can be calculated from molecular modeling. In the molecular modeling, geometric optimization, frequency calculations, and electronic structure calculations are prepared using the Density Functional Theory (DFT) method using the Gaussian 03 software (Gaussian, Inc. 2003). The basis set used for the calculation consists of the Los Alamos National Laboratory double-ζ quality (LANL2DZ) (Wadt and Hay 1985a, Hay and Wadt 1985, Wadt and Hay 1985b) for platinum and 6-311++g** (Hehre, Schlayer, and Pople 1986) for nitrogen, hydrogen, and oxygen atoms.

The LANL2DZ basis set includes a Los Alamos Effective Core Pseudopotential with the double zeta basis set for the outer electrons; 6-31g* is a basis set with a single polarization function while 6-311++g** is a more complete basis set with double polarization (**) and diffuse functions (++). The smaller basis set as shown in the article was able to approximate the bond lengths and bond angles for urea in comparison to other basis sets. The level of theory employed in these calculations is a hybrid B3LYP correlation Hamiltonian functional (Becke 1993). The B3LYP hybrid functional involves the use of a percentage of the Hartree Fock energy in combination with the Vosko, Wilk, and Nusair functional III for local correlation and the Lee, Yang, and Parr functional for non-local correlation. The transition state theory was employed in determining the reaction rate for all the steps mentioned in the two reaction mechanisms. It uses classical mechanics in determining partition functions and, based on the partition functions, the rate constant of the reactions can be determined (Santen and Niemantsverdriet 1995) as shown in:

$$k = \frac{k_b T}{h} \left(\frac{q^{\#}}{\prod\limits_{j=1}^{n} q_j} \right) \exp\left(\frac{-E_i}{RT} \right)$$

Eq. 1

where:

k = the rate constant (s^{-1} for unimolecular reactions and L mol^{-1} s^{-1} for bimolecular reactions)

$q^{\#}$ = the partition function of transition states

q_j = the partition functions of the reactants

E_i = the difference in zero point energies of the reactants and transition state structures (J mol^{-1})

k_b = Boltzmann's constant

h = Planck's constant (J s)

T = 298 K

R = universal gas constant (J mol^{-1} K^{-1}).

The electrocatalyst used for ammonia oxidation is platinum (Pt) so all the calculations regarding the ammonia oxidation mechanism are based on a platinum catalyst surface. A 15 Pt atom cluster was developed (Figure 14) to perform transition state calculations to determine the reaction rates for the individual steps in the Oswin and Salomon mechanism.

Based on the geometric optimization, the preferred sites for the adsorption of an ammonia (NH_3) molecule is the top site (T) of the Pt cluster; the NH_2 intermediate molecule binds at the bridge (B) location; NH and N intermediates prefer the fcc hollow location; and the hydroxide ion (OH$^-$) also prefers to bind on the top location (T) of the Pt cluster. The reaction rates for the Oswin and Salomon mechanism steps were calculated using the transition theory (Table 6). The slowest rate of the reaction indicates that reaction step to the rate determining step (RDS), which can help to explain the interactions of the surface atoms of the Pt cluster with the intermediate molecules. Reaction step 4 in Table 6 indicate that the combination of nitrogen atom on the surface of Pt catalyst to form a nitrogen molecule (N_2) is the rate determining step as its 'k' value is only 1.40 x 10^{-21} s^{-1}.
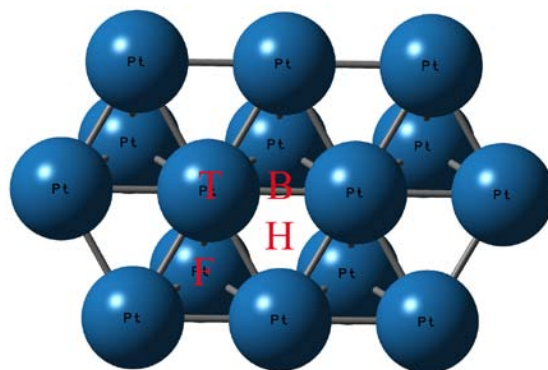
Figure 14. Structure of the Platinum cluster (15 atoms) used in the Gaussian calculations. The different locations for molecules to interact with the Pt cluster is labeled as top site (T), bridge site (B), hcp hollow position (H), and fcc hollow position (F).
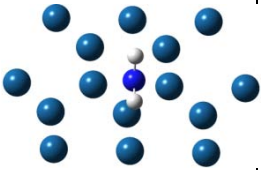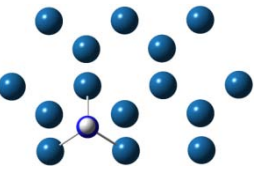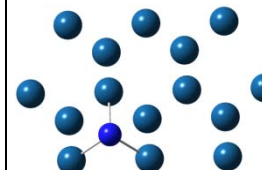
Table 6. Calculated reaction rate for the steps in the Oswin and Salomon ammonia oxidation reaction mechanism.

Reaction steps		Rate constant, k (s^{-1})
1	$PtNH_3 + OH^- \ \square \ \ PtNH_2 + H_2O + e^-$	1.34 x 10^8
2	$PtNH_2 + OH^- \ \square \ \ PtNH + H_2O + e^-$	2.17 x 10^6
3	$PtNH + OH^- \ \square \ \ PtN + H_2O + e^-$	7.33 x 10^2
4	$PtN + PtN \ \square \ \ Pt_2N_2$	1.40 x 10^{-21}

The intermediate molecules such as NH_2, NH, and N as well as NH_3 adsorb on the Pt surface so as to proceed with the electrochemical reaction. The structure of the interaction between the molecule and the Pt surface was optimized using the Gaussian software. Table 7 lists the binding energy or adsorption energy values calculated with and without the inclusion of spin quantum numbers to both Pt atoms and the interacting molecule. Each element has certain number of unpaired electrons, which contributes to its spin quantum number. According to the data in Table 7, the addition of spin quantum numbers in the calculations has brought the adsorption energies closer to the values from Pt slab (bulk) model reported in the literature.

To reproduce the Pt bulk surface for the Gaussian calculations, the size of the Pt cluster was increased to 15, 20, and 25 atoms. This extension of the Pt surface with more atoms will imitate the periodic structure of the bulk Pt. The 15-atom Pt cluster is made of two layers of atoms, similar to the 10-atom Pt cluster. The 20- and 25-atom Pt cluster requires three layers to fit all the atoms. Figure 15 shows the top and side view of the four Pt clusters used in the Gaussian calculations.

Table 7. Adsorption energy for the molecules involved in ammonia electrolysis on Pt cluster.

Molecule	Adsorption Energy (kJ/mol)			
	Adsorbed NH_3	Adsorbed NH_2	Adsorbed NH	Adsorbed N
Illustrate				
Cluster (no spin)	–86	–513	–483	–980
Cluster (spin)	–65	–167	–259	–322
Slab model (ref)	–68	–298	–387	–449

Pt_{10} cluster

Pt_{15} cluster

Pt_{20} cluster
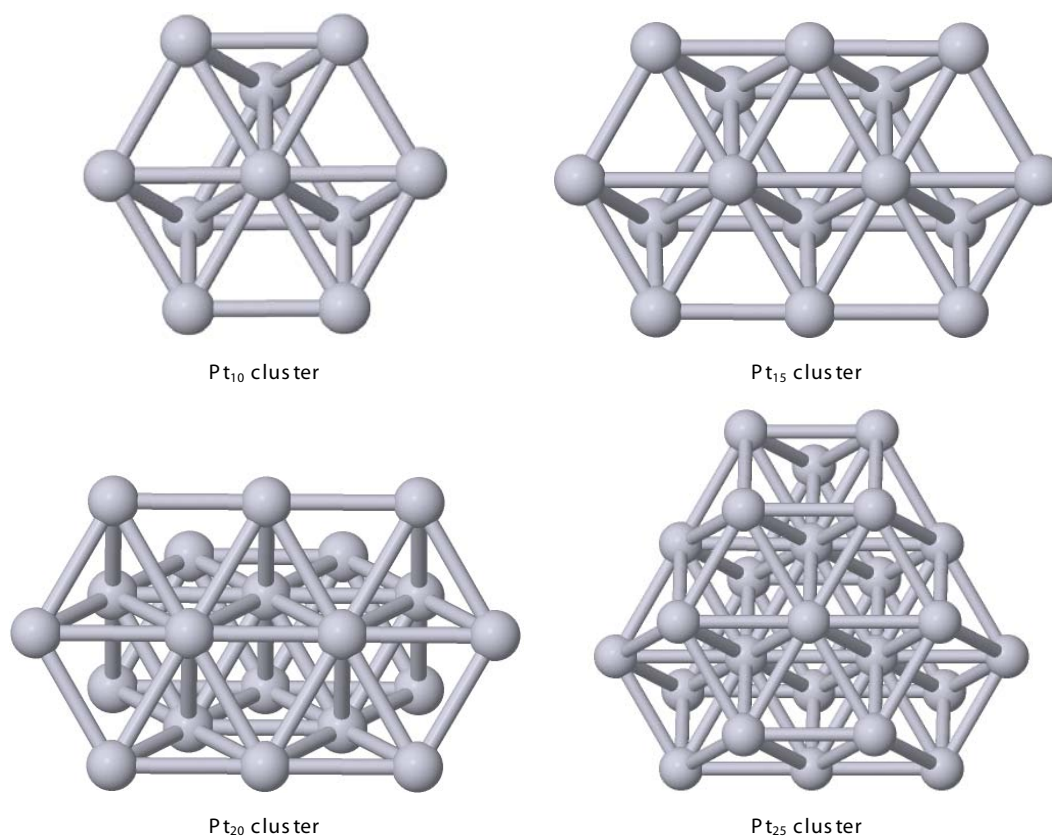
Pt_{25} cluster

Figure 15. Atomic structures of four different Pt clusters (Pt_{10}, Pt_{15}, Pt_{20}, and Pt_{25}). The Pt_{10} and Pt_{15} clusters have two layers of atoms, whereas Pt_{20} and Pt_{25} clusters have three layers of atoms.

The Pt clusters were used in the geometric optimization for the molecules involved in the ammonia electro-oxidation. Table 8 lists the binding energy values for the molecules (NH_3, NH_2, NH, N, OH^-, and H_2O) with Pt clusters such as Pt_{10}, Pt_{15}, Pt_{20}, and Pt_{25}. The data in Table 7 indicate that the binding energy values for the Pt_{20} and Pt_{25} cluster were closer to the slab model. The inclusion of OH^- ion and water molecule is to improve the Gaussian calculations to resemble the real environment during the ammonia electrolysis.

Table 8. Binding energies for the molecules interaction with four different Pt clusters.

Molecule	Binding Energy (kJ/mol)					
	NH_3	NH_2	NH	N	OH	H_2O
Pt_{10}	-56	-150	-274	-354	-178	-17
Pt_{15}	-65	-167	-259	-322	-157	-19
Pt_{20}	-71	-152	-248	-325	-156	-22
Pt_{25}	-75	-179	-314	-350		

The increasing binding energy values for the three layered cluster was expected. The top layer of the Pt_{20} cluster is larger than that of the Pt_{25} cluster, which can be used to calculate multi-molecule adsorption scenarios. Moreover, the time required to calculate using the Pt_{25} cluster is too long compared to the Pt_{20} cluster, so the Pt_{20} cluster will be used for the future Gaussian calculations. From a comparison of the binding energies for the N based molecules with all of the four Pt clusters, it is obvious that N atom has higher affinity with the Pt surface than with the NH_3 molecule. When the water molecule is considered along with the ammonia, which is expected during the electrolysis process, the preferential adsorption of the water's OH^- ion on the Pt surface tends to block or exclude the NH_3 molecule. This reaction pathway information is important for further Gaussian calculations as well as for experimental investigations.

4.2   Recommendations for Phase II

It is recommended that Phase II of this project:

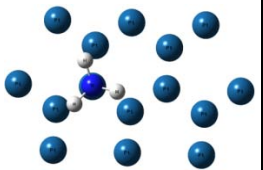- calculate the reaction rates for the steps in the Oswin and Salomon mechanism Using the updated Pt_{20} cluster
- perform the geometry optimization for the N_2H_y molecules (N_2H_2, N_2H_3, and N_2H_4) with the Pt_{20} cluster
- calculate the reaction steps found in the Gerischer and Mauerer mechanism using transition state theory with the Pt_{20} cluster, and determine the reaction rates for each step
- experimentally verify the presence of the intermediates and confirm the molecular model using *in-situ* spectroscopic methods such as Raman, Fourier transform infrared (FT-IR), and x-ray diffraction (XRD) spectroscopy.

4.3   Electro-oxidation of urea

The electrochemical oxidation of urea in alkaline media requires an Ni based catalyst, which has been nickel hydroxide ($Ni(OH)_2$) and nickel oxyhydroxide (NiOOH). The decomposition of urea to ammonia is known

as the hydrolysis of urea, which happens in the presence of a urease enzyme (Estiu and Merz 2004a, Estiu and Metz 2004b, Estiu and Merz 2007, Fearon 1926). There are experimental and theoretical studies performed on the hydrolysis mechanism (Musiani et al. 2001; Barrios and Lippard 2000; Benini 1999; Alexandrova and Jorgensen 2007; Estiu, Suarez, and Merz 2006), but no established publication was found on the electrochemical oxidation of urea in alkaline media.

The investigation of molecular modeling on the urea electro-oxidation was done similarly to the study of the electrochemical oxidation of ammonia mechanism. DFT calculations were performed on the NiOOH catalyst and other molecules involved in the reactions. The level of theory used in the calculations is a hybrid B3LYP correlation Hamiltonian functional (Becke 1993) with the basis set consists of Los Alamos National Laboratory of double-ζ quality (LANL2DZ) (Wadt and Hay 1985a, Hay and Wadt 1985, Wadt and Hay 1985b) for nickel and 6-31 g* (Hehre, Schlayer, and Pople 1986) for carbon, nitrogen, hydrogen, and oxygen atoms. The reaction steps in the mechanism were studied using the transition state theory, where the rate constant for the individual steps are determined (Santen and Niemantsverdriet 1995) using Equation 1.

Figure 16 shows the optimized structure for the interaction of urea molecule with the NiOOH structure. The orientation of the urea molecule towards the NiOOH catalyst will determine the reaction pathway for urea electro-oxidation.
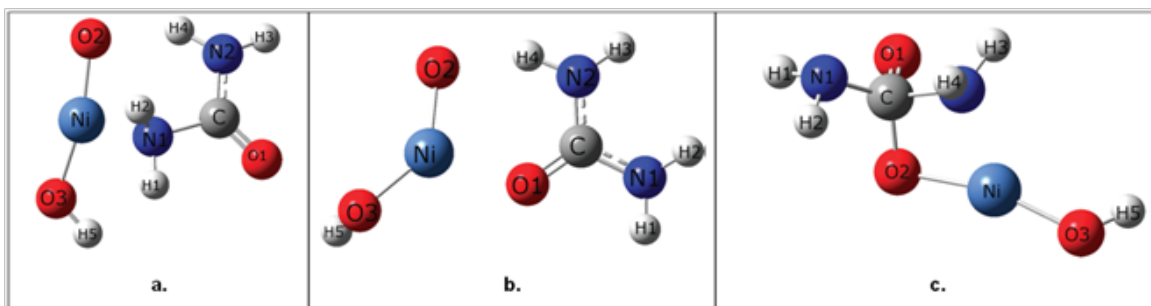
Figure 16. Structural orientation of urea molecule with nickel oxyhydroxide (NiOOH) molecule. (a) Optimized structure of nitrogen coordinated urea on NiOOH, (b) Optimized structure of oxygen coordinated urea on NiOOH, and (c) Optimized structure for bridge-coordinated urea on NiOOH (Daramola, Singh, and Botte 2010).

Three different reaction pathways were proposed for the reaction mechanism of urea electro-oxidation (Daramola, Singh, and Botte 2010). Among those three, the reaction pathway expected to have least resistance based on the rate constants calculated from the transition state theory is:

$$CO(NH_2)_2 + M \rightarrow [M \bullet CO(NH_2)_2]_{ads}$$ Reaction 15

$$[M \bullet CO(NH_2)_2]_{ads} + OH^- \rightarrow [M \bullet CO \bullet NH_2NH)]_{ads} + H_2O + e^-$$ Reaction 16

$$[M \bullet CO \bullet NH_2NH]_{ads} + OH^- \rightarrow [M \bullet CO \bullet NHNH]_{ads} + H_2O + e^-$$ Reaction 17

$$[M \bullet CO \bullet NHNH]_{ads} + OH^- \rightarrow [M \bullet CO \bullet NHN]_{ads} + H_2O + e^-$$ Reaction 18

$$[M \bullet CO \bullet NHN]_{ads} + OH^- \rightarrow [M \bullet CO \bullet N_2]_{ads} + H_2O + e^-$$ Reaction 19

$$[M \bullet CO \bullet N_2]_{ads} + OH^- \rightarrow [M \bullet CO \bullet OH]_{ads} + N_2 + e^-$$ Reaction 20

$$[M \bullet CO \bullet OH]_{ads} + OH^- \rightarrow [M \bullet CO_2]_{ads} + H_2O + e^-$$ Reaction 21

$$[M \bullet CO_2]_{ads} \rightarrow M + CO_2$$ Reaction 22
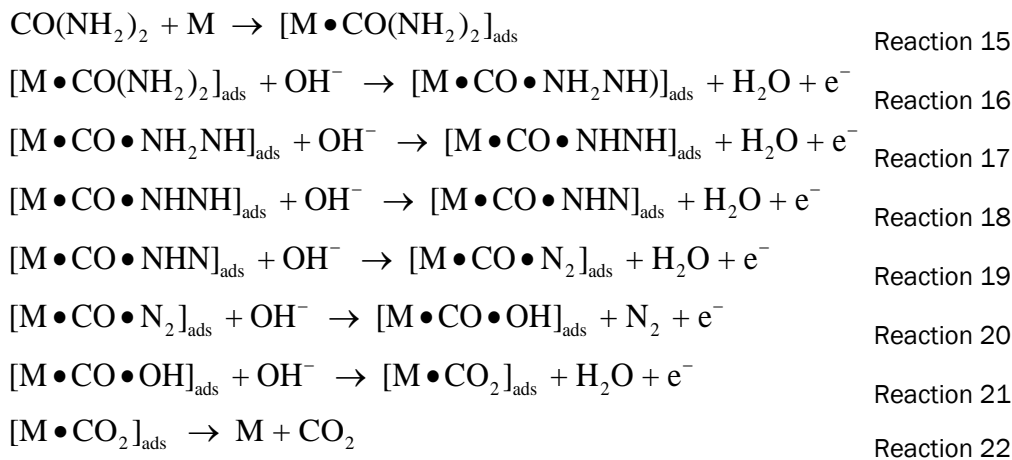
where M stands for the catalyst – nickel oxyhydroxide (NiOOH) molecule.

Table 9 lists the rate constants for the reaction steps listed above were determined using the transition state theory and the calculated 'k' values. Using the reaction rate constants for these reactions, desorption of carbon dioxide (CO_2) from the NiOOH surface is the limiting (slowest) rate determining step. This can also suggest that after the urea molecule is broken down on the NiOOH surface, the carbon-based compounds formed in the process can block the active sites.

Table 9. Kinetic information for the reaction steps involved in urea electrolysis.

Reaction steps	Rate constant, k
$CO(NH_2)_2 + M \rightarrow [M \bullet CO(NH_2)_2]_{ads}$	6.8 L mol^{-1} s^{-1}
$[M \bullet CO(NH_2)_2]_{ads} + OH^- \rightarrow [M \bullet CO \bullet NH_2NH)]_{ads} + H_2O + e^-$	1.4 x 10^{17} L mol^{-1} s^{-1}
$[M \bullet CO \bullet NH_2NH]_{ads} + OH^- \rightarrow [M \bullet CO \bullet NHNH]_{ads} + H_2O + e^-$	1.1 x 10^{17} L mol^{-1} s^{-1}
$[M \bullet CO \bullet NHNH]_{ads} + OH^- \rightarrow [M \bullet CO \bullet NHN]_{ads} + H_2O + e^-$	2.5 x 10^{-4} L mol^{-1} s^{-1}
$[M \bullet CO \bullet NHN]_{ads} + OH^- \rightarrow [M \bullet CO \bullet N_2]_{ads} + H_2O + e^-$	3.6 x 10^{-7} L mol^{-1} s^{-1}
$[M \bullet CO \bullet N_2]_{ads} + OH^- \rightarrow [M \bullet CO \bullet OH]_{ads} + N_2 + e^-$	7.3 x 10^8 L mol^{-1} s^{-1}
$[M \bullet CO \bullet OH]_{ads} + OH^- \rightarrow [M \bullet CO_2]_{ads} + H_2O + e^-$	1.6 L mol^{-1} s^{-1}
$[M \bullet CO_2]_{ads} \rightarrow M + CO_2$	4.3 x 10^{-65} s^{-1}

4.4 Experimental research

The experimental investigation of the reaction mechanism for the electrochemical oxidation of urea involved a cyclic voltammetry study using a rotating disk electrode (RDE). The RDE electrode was prepared by electroplating Ni over a Ti disk (4 mm diameter and 5 mm thick) using a Watt's plating bath. The Ni loading over the Ti disk was 0.5 mg/cm². Figure 17 shows the cyclic voltammogram for the Ni covered Ti electrode in urea solution (0.33 M urea + 5 M KOH) at various scan rates on the RDE electrode.

The urea oxidation peak current and its potential are plotted against the scan rate to determine the kinetic information for the electrochemical oxidation of urea. Figure 18 shows a plot of the urea oxidation peak potential vs. a natural logarithm of the scan rate.
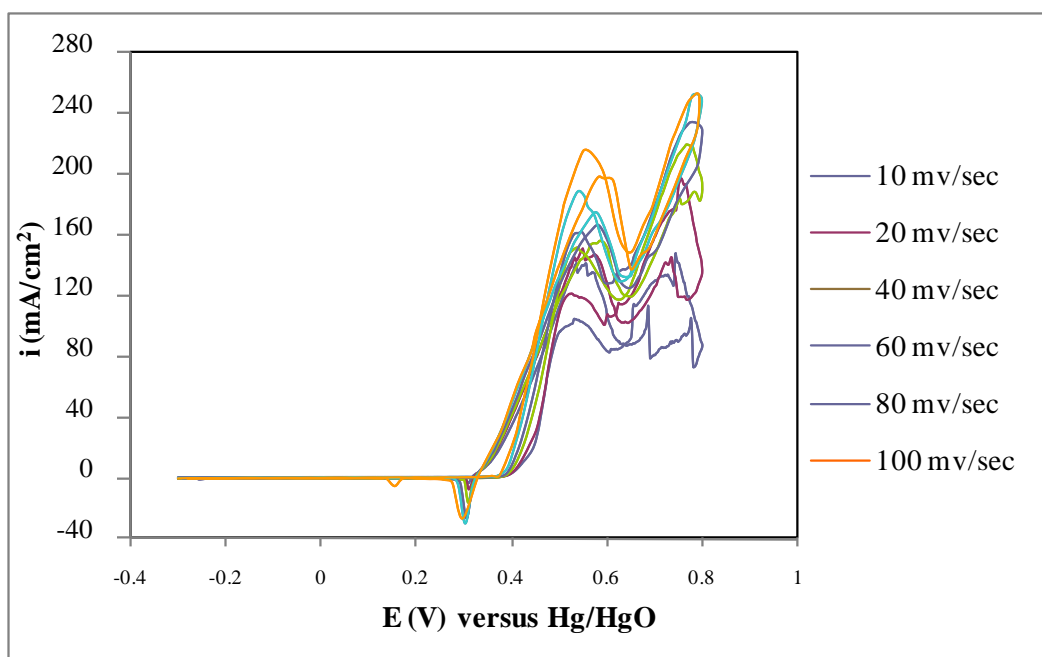
Figure 17. Cyclic voltammogram of Ni (0.5 mg/cm²) covered Ti electrode in urea solution. The urea oxidation peak observed in the forward direction of the scan, whose peak current and oxidation potential varies with the scan rate.
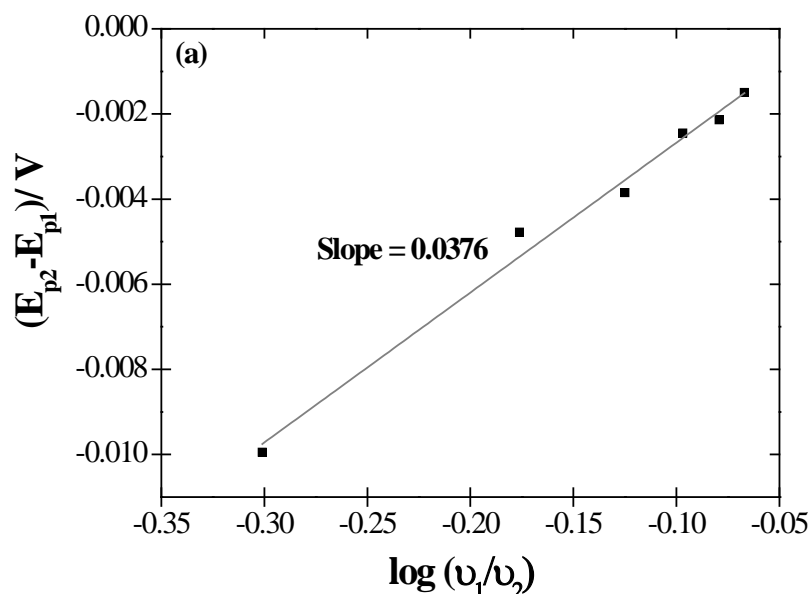
Figure 18. Urea oxidation peak potential as a function of scan rate. Cyclic voltammetry using Ni covered Ti disk in urea solution (0.33 M urea + 5 M KOH).

The transfer coefficient during the oxidation of urea was determined by:

$$E_{p2} - E_{p1} = 0.03 \left(\frac{1}{\alpha n_\circ} \right) \log \left(\frac{\upsilon_1}{\upsilon_2} \right)$$

Eq. 2

where:

E_{p1} = peak potential at v_1 (V)
E_{p2} = peak potential at v_2 (V)
v_1/v_2 = ratio of the potential scan rate
α = transfer coefficient
n_o = number of electrons in the rate determining step ($n_o = 1$).

Using the slope from the plot in Figure 18 along with Equation 2, the transfer coefficient (α) was calculated to be 0.797. The number of electrons involved in the urea oxidation reaction can be calculated using the Randle-Sevcik equation:

$$I_p = 2.99 \text{ x } 10^5 n \left[(1-\alpha) n_\circ \right]^{\frac{1}{2}} AC_o D^{\frac{1}{2}} \upsilon^{\frac{1}{2}}$$

Eq. 3

where:

I_p = peak current (A)
v = potential scan rate (V/s)

$$A = \text{electrode area (cm}^2\text{)}$$
$$C_o = \text{concentration (mol/cm}^3\text{)}$$
$$D = \text{diffusion coefficient (cm}^2\text{/s)}$$
$$n = \text{number of electrons required for the electrochemical reaction}$$

The diffusion coefficient of the urea molecule in water is 7.57×10^{-11} cm^2/s.

Using the transfer coefficient calculated from Equation 2 ($\alpha = 0.797$) and the slope of the plot for peak current versus the square root of the scan rate (Figure 19), the number of electrons (n) required for urea electro-oxidation was found to be 6.064, which approximates to 6 electrons. This value for the number of electrons confirms that the urea oxidation reaction was taking place on the anode electrode as shown in Reaction 4.

4.5 Recommendations for Phase II (reaction mechanisms)

It is recommended that Phase II of this project:

- in molecular modeling, extend a single molecule NiOOH catalyst to the periodic structure similar to Pt clusters in the ammonia electrolysis studies
- study the interaction of each intermediate in the reaction steps of the mechanism with the NiOOH catalyst with periodic structure of NiOOH
- determine the rate constants for all the reaction steps in the mechanism
- experimentally verify the presence of the intermediate and confirm the molecular model using *in-situ* spectroscopic methods such as Raman, FT-IR, and XRD spectroscopy.
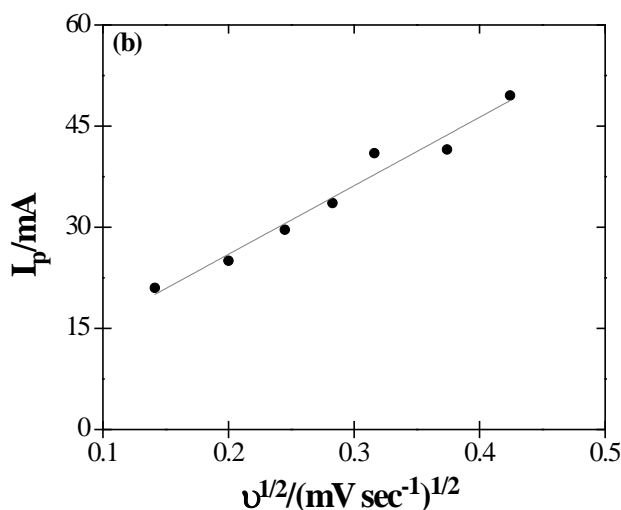
Figure 19. Peak current for urea oxidation as function of the scan rate. The peak current (I_p) for urea oxidation is represented versus the square root of the scan rate (v).

5 Catalyst Development

5.1 Ni-Rh catalyst

The active electrocatalysts for the oxidation of urea were nickel hydroxide and nickel oxyhydroxide. The use of nickel electrodes in the urea electrolysis experiments led to a drop in the activity of the electrode over a period of time. The data in Table 9 (p 28) indicate that the loss in electrocatalytic activity of nickel electrode is attributed to the surface blockage by carbon-based compounds, where the desorption of carbon dioxide from NiOOH surface is the rate determining step for the reaction mechanism of urea electro-oxidation.

This suggests that new and efficient catalysts are required for the electrochemical oxidation of urea in alkaline media. One of the catalysts investigated was a rhodium (Rh) deposited nickel electrode, labeled as Ni-Rh, where Rh has higher affinity to carbon compounds than Ni, and where Rh is expected to remove the surface blockage on Ni sites caused by carbon compounds. For comparison, Figure 20 shows the performance of two electrocatalysts during cyclic voltammetry in urea solution (0.33 M urea + 5 M KOH). The red and purple curves in Figure 20 represent the cyclic voltammograms of Ni and Ni-Rh electrodes, respectively, in blank solution (5 M KOH). A review of the cyclic voltammograms in urea solution reveals that the Ni electrode (blue curve) has lower oxidation currents than the Ni-Rh electrode (green curve). The increase in the urea oxidation current with the Ni-Rh catalyst over the Ni electrode indicates that the presence of Rh along with Ni helps to reduce the effect of carbon compounds blocking the Ni active sites, and to enhance the urea oxidation reaction.

5.2 Large size electrode

The large size Ni-Rh electrodes were prepared using the plating line for the electrolytic cells assembled to form the 50 W GreenBox. The large size electrodes were Ni mesh (#40) shaped as an elongated oval (Figure 21). These electrodes were rinsed thoroughly with deionized water and acetone before being subjected to Rh plating. The composition of the Rh plating bath is 1.27 g/L $RhCl_3$ in 1 M NaCl. Rh was electroplated over the Ni mesh electrodes at a constant cell voltage of 1.566 V. The anode electrodes of the GreenBox were loaded with 70 mg (0.5 mg/cm^2) of Rh, whereas the cathode electrodes were loaded with 140 mg Rh (1.0 mg/cm^2).
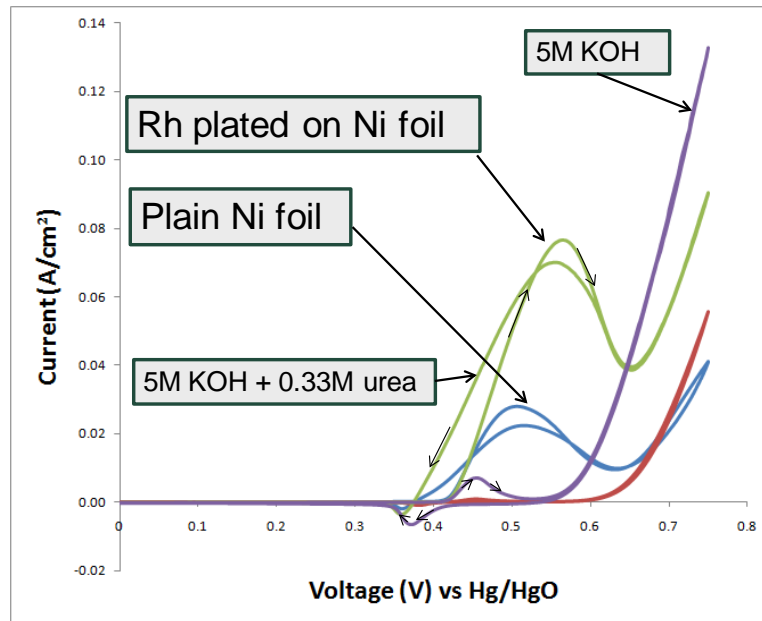
Figure 20. Comparison of cyclic voltammograms of Ni and Ni-Rh electrodes in urea solution. The electrolytes used for this comparison are blank solution (5 M KOH) and urea solution (0.33 M urea + 5 M KOH).
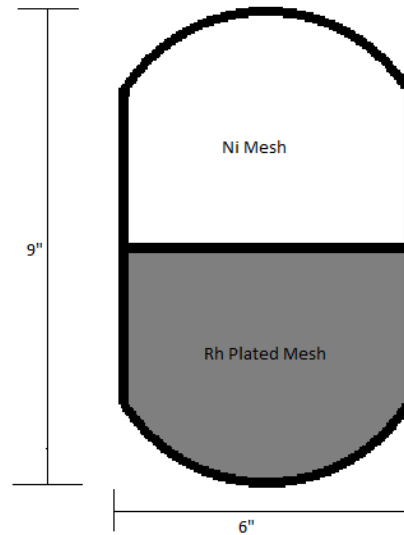
Figure 21. Schematic diagram of the large sized Ni-Rh electrode used in the GreenBox.

The Rh plated Ni electrodes were assembled to form a single cell, which was tested in blank (5 M KOH) and urea (0.33 M urea + 5 M KOH) solutions under an open cell condition. The testing for the cell consisted of increasing the cell voltage from 1.3 to 1.6 V in staircase fashion and observing the oxidation current produced. Figure 22 shows the results from testing a pair of anode/cathode electrodes in blank and urea solution.
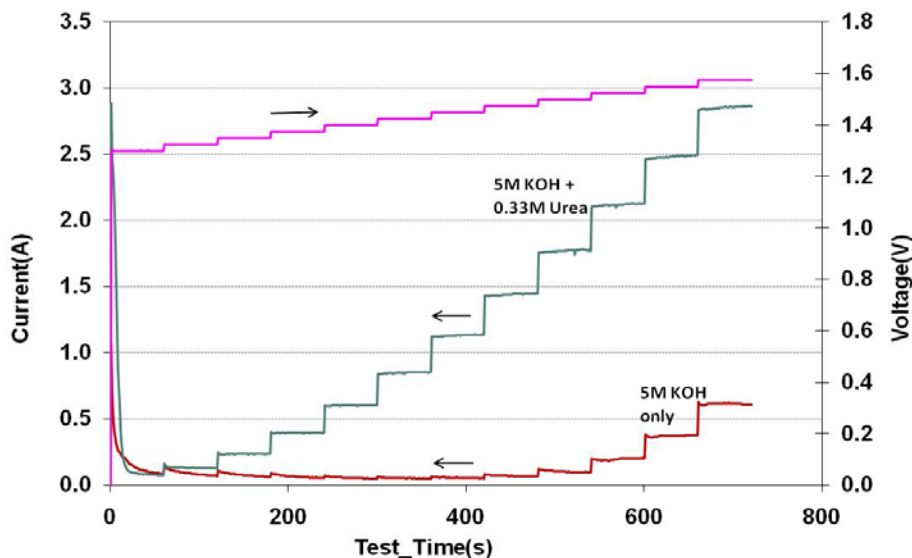
Figure 22. Potentiostatic experiment of an electrolytic cell in blank and urea solution; the anode and cathode is Rh deposited Ni mesh electrode.

The maximum current from the single cell in the urea solution is 2.85 A at 1.575 V. For comparison, Table 10 lists the currents from both blank and urea solutions to illustrate the percentage of actual total current used for the electrolysis of urea; the remainder is taken for water electrolysis at these high cell voltages.

Table 10. Cell voltage and current for the potentiostatic experiment of single cell in blank and urea solution.

Cell voltage (V)	Current (A)		Current efficiency for urea electrolysis
	Blank solution (5 M KOH)	Urea solution (0.33 M + 5 M KOH)	
1.3	0.1	0.1	0
1.35	0.08	0.2366	66%
1.4	0.05	0.8507	94%
1.45	0.07	1.4345	95%
1.5	0.1047	1.771	94%
1.55	0.3373	2.4761	86%
1.575	0.6186	2.8539	78%

5.3   Small sized electrode

The development on the deposition of Rh over Ni electrode was studied using small electrodes of dimensions less than 3 cm x 3 cm. The studies involved optimizing the Rh plating bath and cell voltage for plating only. Investigation of other parameters were left for Phase II of this project.

The cell voltage required to plate Rh over Ni electrodes was investigated on a 3 x 3 cm Ni foil. Since a uniform Rh plating is a very important parameter in the analysis of the catalytic property of this electrode, a plating apparatus was developed to obtain uniform Rh loading over the Ni foil. Figure 23 shows the front and the side view of the apparatus, which was made of polyvinyl chloride (PVC) fittings. The apparatus was submerged in a 600 mL beaker filled with the Rh plating solution. The Rh plating solution flowed through the apparatus, and the streams of solution exited from the apparatus to converge at the center, creating turbulence. Changing the flow rate of the Rh solution through the apparatus leads to variation in the plating voltage.

The counter electrode used in the Rh plating was 5 x 5 cm Pt sheet. The pretreatment for the Ni foil included sand blasting and a rinse with deionized water and acetone`. After drying the Ni foil in the oven, it was further subjected to alkaline cleaning (1 M NaOH) and an acid dip (1 M HCl) to remove any oxide layers formed on the Ni foil surface.
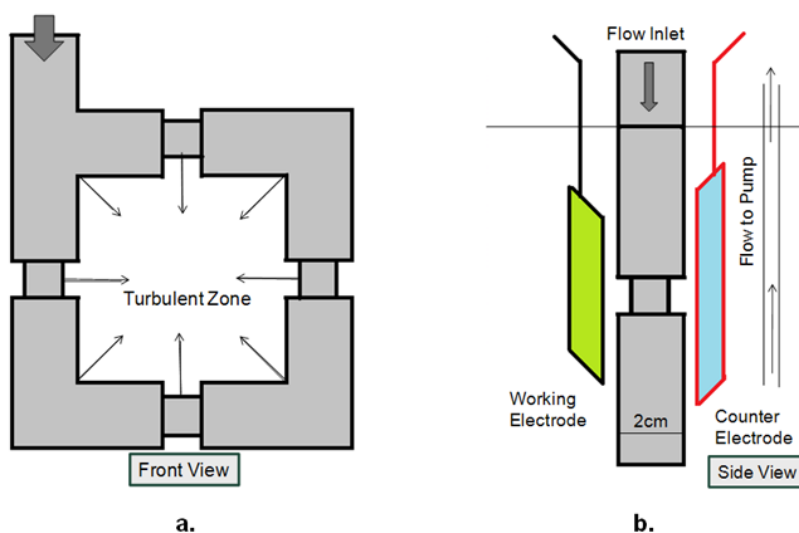
Figure 23. Plating apparatus designed for uniform distribution of Rh over Ni electrode, showing (a) front view of the plating apparatus, and (b) side view of the apparatus (which is immersed in plating solution) and the electrodes.

The Rh was then plated on Ni electrodes at 5 mA/cm² for 352 seconds to apply a plating thickness of 4.6 ± 0.5 mg of Rh. Different cell voltages, ranging from 1.43 to 1.97 V, for the Rh plating was obtained by varying the Rh solution flow rate (0.5 to 1.5 L/min) through the plating apparatus. The plated electrodes were characterized using cyclic voltammetry, X-ray diffraction (XRD) spectroscopy, and (morphologically) using scanning electron microscope (SEM). Figure 24 shows the SEM images of the Rh plated Ni electrodes from different plating voltages.

The SEM images of the Rh plating indicate that applying low cell voltages in the Rh plating process results in full coverage of Rh over the Ni foil and a cracking of the deposited Rh sheet. However, applying high cell voltage in the Rh plating process results in the formation of Rh nodules covering the Ni foil completely. Figure 25 shows the XRD spectra for these Rh plated Ni foils, which indicate the presence of an Rh (111) crystal plane.

The broadness of Rh(111) peak suggests that the (111) planes on the Rh deposit are not well defined, and that its ability to catalyze urea electrooxidation must be further examined. Preliminary results from the urea electrolysis using these Rh plated electrodes suggest that a higher intensity Rh(111) peak in the XRD spectra results in a lower charge for the urea oxidation (Figure 26).

The relation between the Rh(111) peak intensity and the charge for urea oxidation might indicate that the deposited Rh has more coverage over the Ni surface. This high Rh coverage would hinder the electrochemical interaction between the urea molecule and the Ni sites. Figure 27 shows the relationship between the urea oxidation charge and the Ni(111) peak intensity, which supports the findings shown in Figure 26, with lower Ni(111) peak intensity and less urea oxidation charge. In other words, the Ni(111) peak intensity might have been lowered with more Rh coverage. This will require further study in the Phase II of this project to confirm these findings.

5.4 Ni-Co hydroxide catalyst

One of the concerns during the electrochemical oxidation of urea is the overpotential required for this reaction. Theoretically, the oxidation of urea (Reaction 4) requires -0.46 V vs. SHE, but this reaction will require 0.45 V vs. SHE on pure Ni surface, indicating a large overpotential. The large overpotential for urea oxidation provides room for a secondary reaction such as the oxygen evolution reaction (OER).
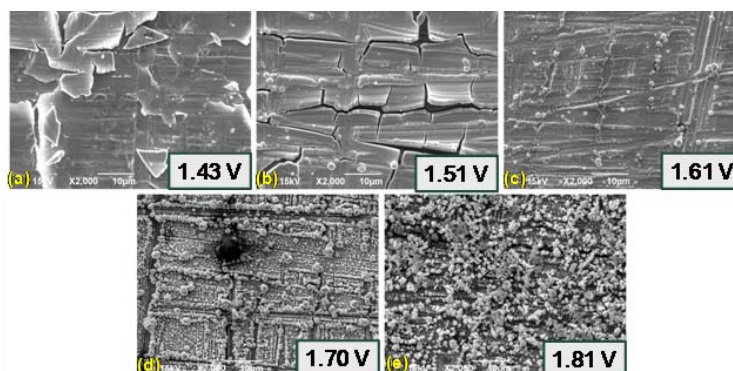
Figure 24. SEM images of Rh plated Ni foil electrodes. The Rh was plated on the Ni foil electrodes at cell voltages of (a) 1.43 V, (b) 1.51 V, (c) 1.61 V, (d) 1.70 V, and (e) 1.81 V.
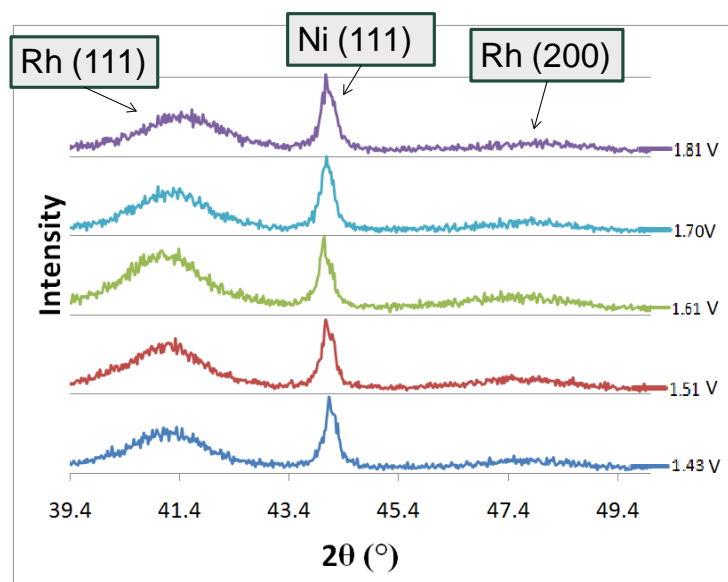
Figure 25. XRD spectra of Rh deposited Ni foil. The presence of Rh(111), Rh(200), and Ni(111) are observed in these spectra.
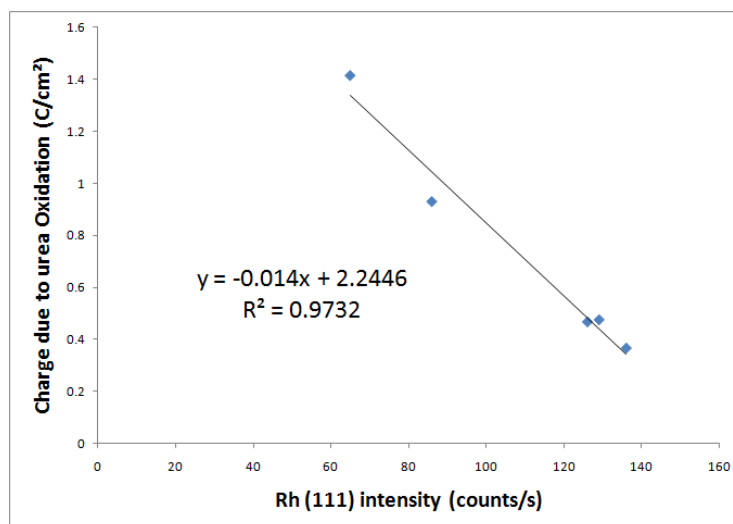
Figure 26. Urea oxidation charge as a function of Rh(111) peak intensity. The amount of Rh(111) deposited have influenced the amount of urea molecules oxidized.
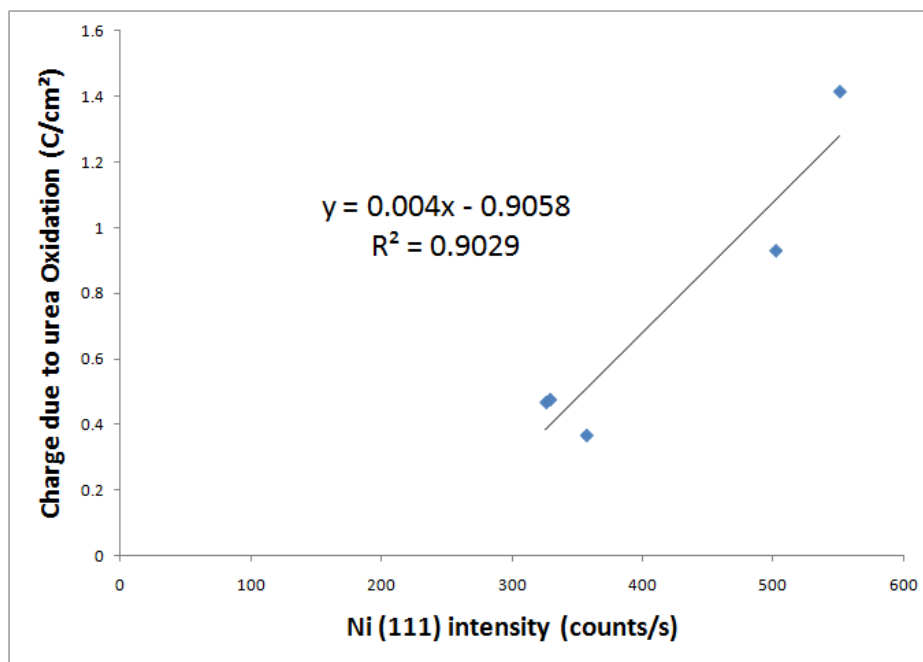
Figure 27. Urea oxidation charge as a function of Ni(111) peak intensity. The coverage of Rh on Ni surface has influenced the amount of urea molecules oxidized.

The use of cobalt (Co) along with the $Ni(OH)_2$ catalyst was investigated to avoid the OER. (In previous research [Vidotti et al. 2008], nickel-cobalt hydroxide has been used in urea determination and OER prevention.) Partial substitution of Ni in bulk $Ni(OH)_2$ with Co has shown to improve the electrochemical property of the catalyst (Pickett and Maloy 1978).

A study was done to determine the composition of the nickel-cobalt hydroxide, so that the new catalyst would reduce the overpotential for urea oxidation. The catalyst (nickel-cobalt bimetallic hydroxide) was co-deposited on a pretreated Ti substrate. The pretreatment steps for the Ti substrate involved ultrasonic cleaning with liquid soap solution, 0.01 M potassium hydroxide, and 0.01 M nitric acid, which was followed by rinsing with distilled water and acetone. After cleaning the Ti surface, it was sandblasted and then again ultrasonically cleaned with distilled water and acetone. Table 11 lists the composition of the solution used to deposit six catalyst samples with different compositions of nickel-cobalt hydroxide. The composition of the nickel-cobalt bimetallic hydroxide was changed by varying the concentration of the nitrate salt of the corresponding metal in the supporting electrolyte (0.1 M KNO_3).

Table 11. Composition of deposition solution for nickel-cobalt hydroxide catalyst.

Samples	Composition of deposition solution
Sample A	$0.1 \text{ M KNO}_3 + 0.01 \text{ M Ni(NO}_3)_2$
Sample B	$0.1 \text{ M KNO}_3 + 0.009 \text{ M Ni(NO}_3)_2 + 0.001 \text{ M Co(NO}_3)_2$
Sample C	$0.1 \text{ M KNO}_3 + 0.008 \text{ M Ni(NO}_3)_2 + 0.002 \text{ M Co(NO}_3)_2$
Sample D	$0.1 \text{ M KNO}_3 + 0.005 \text{ M Ni(NO}_3)_2 + 0.005 \text{ M Co(NO}_3)_2$
Sample E	$0.1 \text{ M KNO}_3 + 0.002 \text{ M Ni(NO}_3)_2 + 0.008 \text{ M Co(NO}_3)_2$
Sample F	$0.1 \text{ M KNO}_3 + 0.01 \text{ M Co(NO}_3)_2$

The surface of the samples was characterized using SEM. Figure 28 shows the SEM images of the six deposited samples. The addition of Co to the $Ni(OH)_2$ catalyst resulted in a breakdown of the $Ni(OH)_2$ films on the Ti substrate. An increase in Co content up to 43% (atomic weight) in the nickel-cobalt hydroxide catalyst resulted in smaller fragmentation of the catalyst. However, beyond 73% (atomic weight) of Co in the bimetallic hydroxide catalyst, large changes were observed; the film structures of the catalyst became increasing dense.
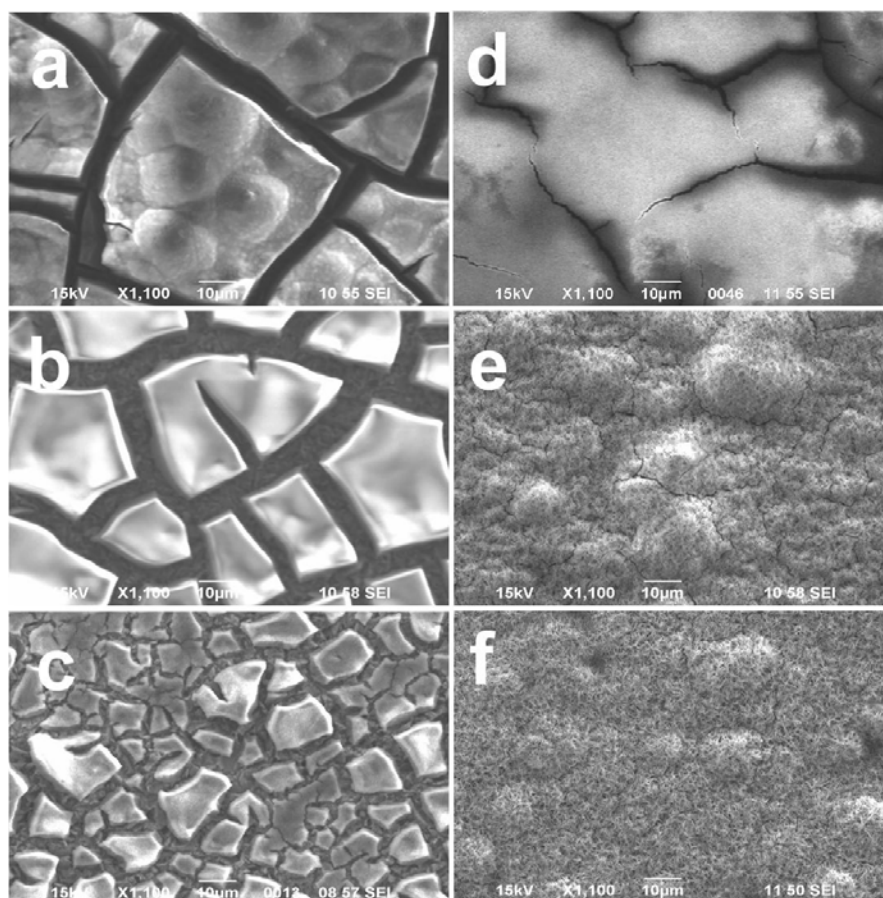
Figure 28. SEM images of the nickel-cobalt hydroxide electrodes. (a) Sample A, (b) Sample B, (c) Sample C, (d) Sample D, (e) Sample E, and (f) Sample F.

The chemical composition of the samples was expected to follow the solution compositions listed in Table 11, but there were appreciable changes in the composition of the catalyst. Electrochemical characterization of the six electrodes involves cyclic voltammetry in blank (5 M KOH) and urea (0.33 M urea + 5 M KOH) solutions. The onset potential for the electrochemical oxidation of urea was determined for the six electrodes. Figure 29 shows the onset potential for urea oxidation as a function of Co content in the bimetallic hydroxide catalyst. As Figure 29 shows, as the Co content in the catalyst increased of up to 43% (atomic weight), the onset potential moved towards lower potential values, which indicates a lower overpotential for urea oxidation. However, beyond 43% (atomic weight) of Co in the catalyst, the onset potential increased towards that of the pure $Ni(OH)_2$ electrode behavior because Co or $Co(OH)_2$ is not an effective catalyst for the electro-oxidation of urea.

The addition of 43% (atomic weight) of Co to the pure $Ni(OH)_2$ catalyst lowered the onset potential for urea oxidation by 150 mV. Constant cell voltage experiments were performed, between 1.35 and 1.6 V for Sample A (pure $Ni(OH)_2$) and Sample C (43% Co in $Ni(OH)_2$) with blank and urea solutions. Catalyst containing Co inhibited the water electrolysis process and enhanced the urea electrolysis efficiency.
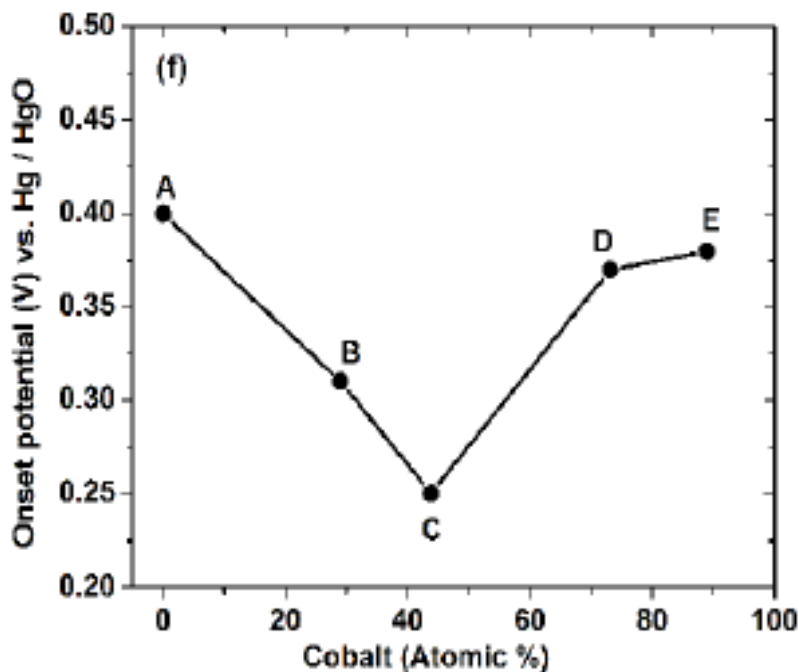
Figure 29. Onset potential for urea oxidation as function of Co content in the bimetallic catalyst. Sample C with 43% Co in the catalyst has the lowest onset potential.

5.5 Ni(OH)$_2$ nanosheets

The field of nanoscience and nanotechnology has helped in the production of efficient catalysts for various applications at reduced catalyst quantity and higher catalytic efficiency. On this basis, the synthesis of two-dimensional (2D) Ni(OH)$_2$ nanosheets was studied to improve the current density of the urea electrolysis process and to reduce the onset potential of the urea oxidation. The synthesis of layered Ni(OH)$_2$ nanosheets required mixing 5 mmol of sodium dodecyl sulfate (SDS), 2 mmol of nickel nitrate hexahydrate (Ni(NO$_3$)$_2$ 6H$_2$O), and 12 mmol of hexamethylenetetramine (HMT) with 100 mL of water. This mixture was allowed to react in a sealed Teflon vessel at 90 °C for 24 hrs.

A green precipitate was obtained after the product solution was centrifuged at 10,000 rpm for 30 minutes. The layered Ni(OH)$_2$ was washed thoroughly with distilled water and acetone by shaking and centrifuge. Figure 30 shows the XRD pattern of the dried layered nickel hydroxide, which displays a number of Miller indices "*OON*-type" reflections, suggesting the synthesized Ni(OH)$_2$ were ordered along the layer stacking direction. Using the reflection angles and Bragg's law, the interlayer distance along the c axis was calculated to be 2.67 nm.
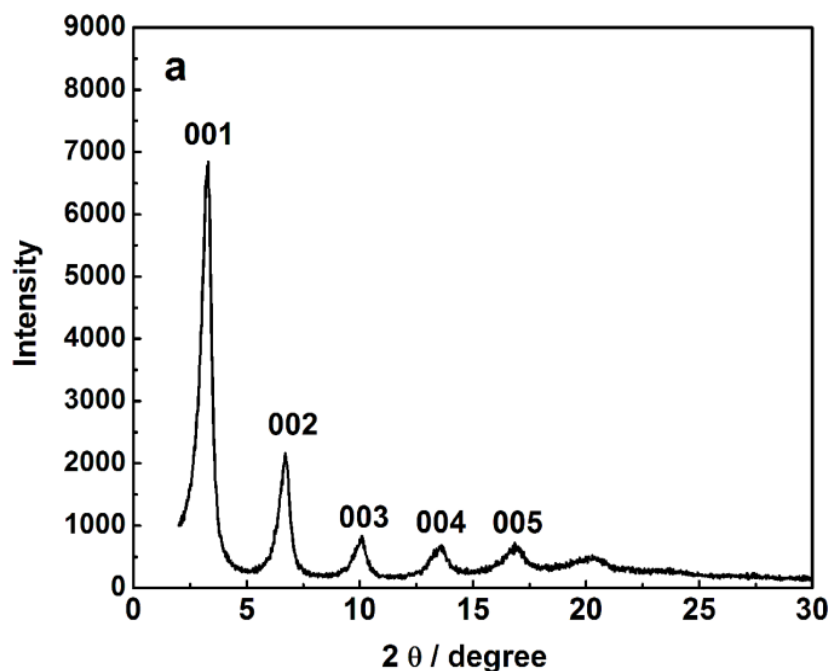
Figure 30. XRD pattern of the SDS intercalated layered nickel hydroxide (Wang, Yan, and Botte 2011).

Adding the layered Ni(OH)$_2$ to a formamide solution and stirring at 200 rpm for 4 days resulted in exfoliated layered Ni(OH)$_2$. The solution with the suspended exfoliated Ni(OH)$_2$ was centrifuged at 2000 rpm to obtain nanosheets of the Ni(OH)$_2$ in the supernatant solution. The atomic force microscopy (AFM) was used to study the morphology of the Ni(OH)$_2$ nanosheets. Figure 31 shows the AFM image of the Ni(OH)$_2$ nanosheets, which has a lateral size ranging from a few hundred nanometers to a micrometer. The thickness of the exfoliated Ni(OH)$_2$ nanosheets was around 1 nm.

The catalytic activity of the Ni(OH)$_2$ nanosheets was analyzed by cyclic voltammetry. The electrochemical experiments were performed with an electrode developed by attaching the Ni(OH)$_2$ nanosheets on the glassy carbon electrode by Teflon binder. For comparison, Figure 32 shows the cyclic voltammograms of the Ni(OH)$_2$ nanosheets in blank (5 M KOH) and urea (0.33 M urea + 5 M KOH) solution vs. the Ni(OH)$_2$ powder.
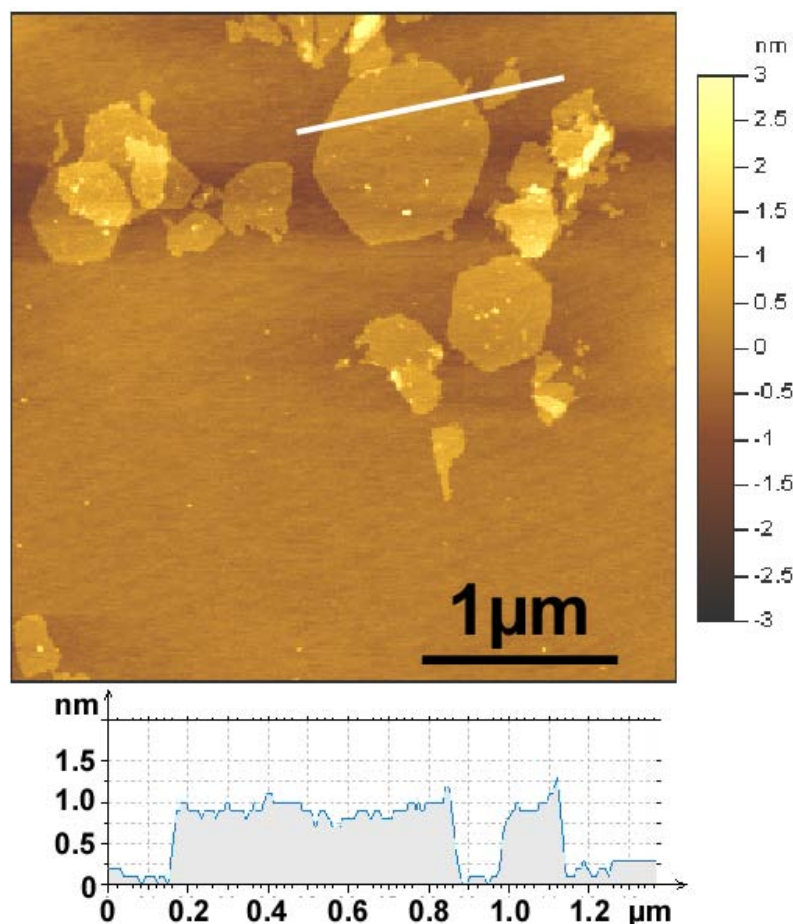
Figure 31. AFM image of the exfoliated layered nickel hydroxide nanosheets. The lateral size of the nanosheets ranged from a few hundred nanometers to a micrometer and the thickness was around 1 nm (Wang, Yan, and Botte 2011).
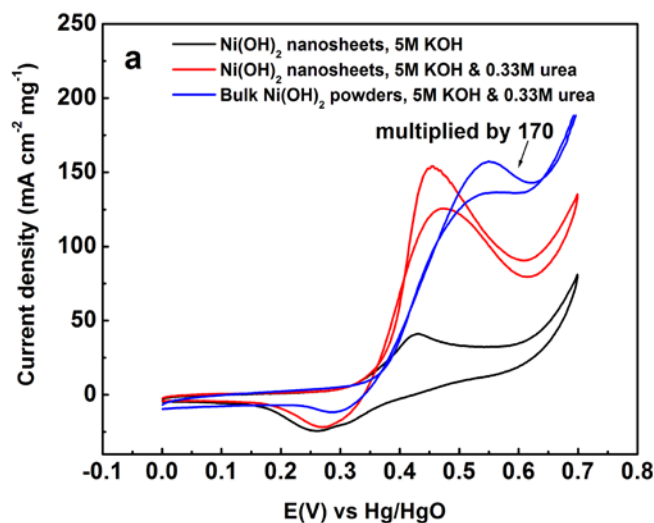
Figure 32. Comparison of cyclic voltammograms of the Ni(OH)$_2$ nanosheets modified glassy carbon electrode and bulk Ni(OH)$_2$ powder modified glassy carbon electrode (Wang, Yan, and Botte 2011).

The peak potential for the urea oxidation was shifted by 100 mV in the negative direction for the Ni(OH)$_2$ nanosheet modified electrode on comparison with the bulk Ni(OH)$_2$ powders. The oxidation current for the Ni(OH)$_2$ nanosheets modified electrode was 154 mA cm^{-2} mg^{-1}, which was 170 times larger than the bulk Ni(OH)$_2$ powder. The Ni(OH)$_2$ nanosheets modified glassy carbon electrode was a better performing catalyst as it lowered the urea oxidation potential by at least 300 mV from the noble metal catalysts (Boggs, King, and Botte 2009; Simka, Piotrowski, and Nawrat 2007; Simka et al. 2009).

5.6   Recommendations for Phase II (catalyst development)

It is recommended that Phase II of this study:

- establish Rh plating conditions on Ni electrodes to obtain predominantly Rh(111), which would enhance urea electro-oxidation
- scale up the new Rh plating process for preferred crystal plane on the Ni electrode to the large extended oval shaped electrodes for use in the GreenBox
- scale up of the new catalysts such as nickel-cobalt bimetallic hydroxide to the large sized electrodes to be used in the GreenBox
- transfer the Ni(OH)$_2$ nanosheets to the large sized electrodes for use in the GreenBox
- use the Ni(OH)$_2$ nanosheets as a catalyst support material for other noble metal-based catalyst for ammonia electrolysis, which would apply to large sized electrodes for the GreenBox application.

6 Application of Ammonia and Urea Electrolysis in Wastewater Remediation

This project was undertaken to investigate the application of electrolysis of ammonia and urea as a hydrogen fuel source in support the silent camp project. The process developed in this work has great potential to provide an efficient fuel source for PEM fuel cells. However, the electrolysis of ammonia and urea also has broad applications in military and civilian applications related to wastewater remediation.

As the global population rises (to an expected 9 billion by 2050), the demand for potable water will increase, while access to fresh water will decrease. At the same time, wastewater quantities will exceed the capacity of existing wastewater management facilities, requiring facility expansions and quality improvements in expelled water.

Wastewater treatment plants (WWTPs) are net users of energy. In the United States WWTPs consume an average estimated 21 billion kWh/yr, which represents 3% of the electric load in the United States. Energy costs can account for 30% of the total operation and maintenance (O&M) costs of WWTPs. Continual increases in energy costs in the United States affect wastewater treatment plants just as they do other facilities. Furthermore, as populations grow and environmental requirements become more stringent, demand for electricity at such plants is expected to grow by approximately 20% over the next 15 years. Thus, energy conservation is an issue of increasing importance to WWTPs.

Secondary treatment processes (for the removal of organic matter and nitrogen) in WWTPs are responsible for about 60% of the energy consumption in WWTPs. The removal of ammonia (through nitrification/denitrification technology) consumes an average of 1073 kWh per million gallon (MG) of water. This value is significant considering that cities with populations over 2.5 million people commonly require WWTPs with capacities that exceed 400 million gallon per day (MGD). Currently, wastewater treatment solutions for ammonia (biological and chemical treatments) consume a significant amount of energy (3.2 kWh per kg of ammonia removed); have high operational costs ($4 per lb of ammonia removed); require significant capital investment ($658,000 per MGD), are not flexible to tighter emissions regulations; and are large in size. (Size alone makes

such systems less feasible in urban areas where there is limited room for expansion.)

Both traditional and the ammonia/urea remediation systems require additional support systems for their operational execution (SBW 2002). The GreenBox system offers significant advantages over those systems:

- The GreenBox system is compact in size, and is expected to provide superior efficiencies due to reduction of pumping length runs, and power for these systems.
- The GreenBox minimizes associated maintenance and upkeep with reduced numbers of storage vessels and smaller floor space requirements.
- The experimental GreenBox process offers significant energy efficiencies over conventional ammonia remediation technologies. The data in Table 1 (p 5) indicate that the GreenBox process requires between 9 and 17 Wh of energy to recover 1 g of hydrogen gas, depending on pH and concentration of ammonia. This process destroys 5.67-grams of ammonia (i.e., from Reaction 3, 2[17/6]), and therefore consumes only 1.59 to 3.00 Wh for each gram of ammonia destroyed. This process is clearly competitive with the conventional remediation technology, which requires 3.2 to 5.0 Wh to remove 1 g of ammonia (SBW 2002).
- A further advantage of the GreenBox process is that, in addition to destroying ammonia, it liberates hydrogen gas, which can then be used as fuel in a PEM fuel cell.
- Typically, commercial PEM fuel cells can produce ~14.0 Wh of useful electricity for each gram of input hydrogen. Since the GreenBox process requires between 9 and 17 Wh to produce a gram of hydrogen, the energy produced by the PEM/GreenBox configuration *may* represent a net gain of electrical power. (Note that this does not account for potential parasitic losses in the GreenBox process.)

Thus GreenBox technology can efficiently destroy ammonia while returning in kind the initial electro-decomposition energy requirements and in doing so, become a potential net producer of energy. This remediation of ammonia through the electrolysis process offers several significant advantages over all other ammonia wastewater remediation technologies (air stripping, SHARON,* DEMON®,† etc). No other wastewater technology

---

* SHARON (**S**ingle reactor system for **H**igh activity **A**mmonium **R**emoval **O**ver **N**itrite, see: http://www.dep.state.pa.us/dep/deputate/watermgt/wsm/wsm_tao/InnovTech/ProjReviews/SharonHiRate.htm

† DEMON (**DE**-am**MON**iafication Process), see http://grontmij.com/demon

presently has the capability to produce an emission free (hydrogen) energy source. The availability of a pure hydrogen fuel source allows the practical application of PEM fuel cells and ultra high efficient underwater hydrogen combustion.

Ammonia and urea electrolysis are platform technologies that have significant relevance to maintain water resources. Successful development of the proposed technology will yield an efficient system for onsite treatment that is simple to operate while providing the added benefit of producing fuels for electrical and thermal energy generation. The ammonia and urea electrolysis technologies will benefit the DoD by reducing the costs, logistical burden, and risks associated with wastewater management at FOBs and other expeditionary outposts.

7 Conclusions and Recommendations

7.1 Conclusions

The electrolysis of ammonia and urea has shown the potential to generate a high value fuel from a wastewater source. Phase I of this project focused on determining the kinetics and operating parameters required for the scale up of ammonia and urea electrolyzers, specifically, by improving the electrochemical reaction rates for the oxidation of ammonia and urea. Progress was made by focusing on three important areas: improvement on the fundamental knowledge of the mechanisms of reactions, catalyst development, and construction and scale up of a bench scale electrolyzer.

7.1.1 Improvement on the fundamental knowledge of the mechanisms of reactions

Experiment has shown that the ammonia electrolysis process consumes less energy to produce pure hydrogen than urea and water electrolysis. A commercial water electrolyzer requires 49.75 Wh per gram of hydrogen. On the other hand, an ammonia electrolytic cell with Pt-Rh catalyst on carbon fiber consumed only 8.6 Wh per gram of hydrogen at 50 °C and 5 M NH_3. Even the highest energy consuming value for the ammonia electrolytic cell (Pt-Ir catalyst) was 17.3 Wh per gram of H_2 at 25 °C and 1 M NH_3. Energy savings using ammonia electrolysis is at least 65.1% more efficient when compared to that of water electrolysis. In the case of urea electrolysis, an electrolyzer with Rh plated Ni mesh electrode consumed 34.96 Wh to produce 1 g of hydrogen, which is still 29.7% more energy efficient than water electrolysis.

This work performed fundamental studies using molecular modeling methods and basic electrochemistry techniques coupled with analytical methods to evaluate the reaction mechanisms for the electrochemical oxidation of ammonia and urea. In molecular modeling, there are two established reaction mechanisms for ammonia electro-oxidation (Oswin and Salomon, and Gerischer and Mauerer). The rate constants for the reaction steps postulated in the Oswin and Salomon mechanism were calculated using transition state theory. A Pt catalyst model was developed from a single molecule to a periodic structure (Pt_{20} cluster) with physical properties similar to the bulk Pt surface. This Pt surface would be extensively used in future calculations to confirm the reaction mechanism for ammonia electrolysis.

This work proposed a reaction mechanism for urea electrolysis using the molecular modeling calculations with a single molecule of NiOOH catalyst. The rate determining step predicted from transition state theory calculations is the desorption carbon dioxide from the NiOOH surface, suggesting the carbon-based compounds could be blocking the Ni active sites from urea oxidation. It is anticipated that, in Phase II of this project, the structure of the active catalyst for urea oxidation (NiOOH) would be modeled to better include the bulk Ni surface details and so to provide a better estimate of reaction rate constant values, which are in closer agreement with the experimental data.

This work designed an electrolytic cell for ammonia and urea electrolysis with large rectangular shaped planar electrodes, and then changed the electrode design to an extended oval shape to allow easier removal of gases and to avoid the gas build up leading to high back pressure. The electrodes were assembled to form a single electrolytic cell and the urea electrolysis was performed to verify the catalytic activity of the electrode (Ni-Rh). The optimum conditions for hydrogen generation with the single cell system in 0.33 M urea + 5 M KOH solution was to operate the cell at 1.6 V with the anode electrolyte flow rate of 7.8 mL/min and the cathode electrolyte flow rate was maintained at 120 mL/min. The optimum conditions for the single cell electrolyzer to remove urea from the electrolyte were: (1) to maintain the cell voltage at 1.6 V, and (2) to maintain an electrolyte flow rate of 1.1 mL/min for the anode, and 120 mL/min for the cathode.

7.1.2 Catalyst development

The active catalyst for urea electro-oxidation is the $Ni(OH)_2$ and NiOOH redox couple. During the electrolysis, the observed catalyst activity was reduced and researchers predicted surface blockage by carbon compounds. The presence of Rh along with Ni has enhanced the urea oxidation current. Platinum group metals have higher affinity towards carbon compounds, so Rh in the Ni-Rh catalyst helps to preferentially remove the carbon compounds from Ni active sites thereby enhancing the urea oxidation current.

Phase I of this project developed two new catalyst materials. Nickel-cobalt bimetallic hydroxide was synthesized electrochemically. The addition of 43% (atomic weight) of Co to the $Ni(OH)_2$ will lower the onset potential for urea oxidation. The reduction in onset potential for urea indicates the cell voltage for the electrode containing nickel-cobalt hydroxide will be less than $Ni(OH)_2$ electrodes.

Recent progress in the catalyst development was the formation of $Ni(OH)_2$ nanosheets. The $Ni(OH)_2$ is a layered compound that can be exfoliated to form nanosheets. These $Ni(OH)_2$ nanosheets have a thickness of approximately 1 nm and a lateral size that varies between a few hundred nanometers and a micrometer. A $Ni(OH)_2$ nanosheets modified glassy carbon electrode displayed urea oxidation current 170 times larger than $Ni(OH)_2$ powder modified glassy carbon electrode. The surface area on the $Ni(OH)_2$ nanosheets catalyst is very large. It is anticipated that Phase II of this project will determine the capability of the $Ni(OH)_2$ nanosheets as catalyst and as a support material for other catalysts.

Furthermore, the new developments in the synthesis of nickel nanosheets can be coupled with the ammonia and urea electrolysis technology. This work concludes that the nickel nanosheets will support the electrocatalysts used in the ammonia electrolyzer, and in turn has the potential to reduce the energy consumption during the electrolysis of ammonia to less than 8.6 Wh/g of hydrogen, thus providing higher net energy when combined with a hydrogen fuel cell.

7.1.3 Construction and scale up of a bench scale electrolyzer

A highlight of the Phase I research work was the construction and testing of a 50 W electrolyzer known as the GreenBox. This electrolyzer reflects the linear scalability of the ammonia and urea electrolysis systems as well as the advancement in the catalyst material development. Assembly of 10 single electrolytic cells into a stack forms a 50 W GreenBox system. The operation and testing of the GreenBox requires constant monitoring of such parameters as anode electrolyte flow rate, cathode electrolyte flow rate, temperature, pH of the electrolyte, cell voltage, current, pressure, and electrolyte composition. Consequently, a test stand was custom built to meet the requirements of operating, monitoring, and digital data acquisition of the GreenBox during electrolysis. It is anticipated that Phase II of this project will include a more detailed experimental analysis of the operation of the 50 W GreenBox.

7.2 Recommendations for Phase II or future work

In the following areas, it is recommended that Phase II of this project:

- *Electrolysis of ammonia and urea*
    - o Use nickel contacts in the preparation of electrodes for the future experiments.
    - o Use the nanostructured catalyst such as $Ni(OH)_2$ nanosheets as catalyst and possible support material in the future electrode generations.
- *Test of 50 W GreenBox*
    - o In future experiments, consider other parameters related to the urea electrolysis in the GreenBox system. (Determination of the effect of the following variables is currently planned: temperature, current, flow rates, electrolyte concentration, and urea concentration.)
- *Reaction mechanisms*
    - o Calculate the reaction rates for the elementary steps in the Oswin and Salomon and the Gerischer and Mauerer mechanisms using the Pt_{20} cluster modeled.
    - o Build a NiOOH cluster structure that is more representative of a larger nickel electrode to provide a better understanding of the oxidation of urea.
    - o Verify experimentally the presence of the intermediates for both ammonia and urea electrolysis, and validate the molecular models using *in-situ* spectroscopic methods such as Raman, FT-IR, and XRD spectroscopy.
- *Catalyst development*
    - o Establish Rh plating conditions on Ni electrodes to obtain predominantly Rh(111), which would enhance urea electro-oxidation.
    - o Scale up the new Rh plating process for preferred crystal plane on the Ni electrode to the large extended oval shaped electrodes for use in the GreenBox.
    - o Scale up of the new catalysts such as nickel-cobalt bimetallic hydroxide, to the large sized electrodes to be used in the GreenBox.
    - o Transfer the $Ni(OH)_2$ nanosheets to the large sized electrodes for use in the GreenBox.
    - o Use the $Ni(OH)_2$ nanosheets as catalyst support material for other noble metal based catalyst for ammonia electrolysis, which would transfer to large sized electrodes for the GreenBox application.

Acronyms and Abbreviations

Term	Definition
AEC	ammonia electrolytic cell
AFM	atomic force microscopy
ANSI	American National Standards Institute
CERL	Construction Engineering Research Laboratory
DFT	Density Functional Theory
ERDC	Engineer Research and Development Center
FC	flow control (valve)
FT-IR	Fourier transform infrared (spectroscopy)
HMT	hexamethylenetetramine
HQUSACE	Headquarters, U.S. Army Corps of Engineers
LFM	liquid flow meter)
MG	million gallons
MGD	million gal/day
NAE	National Academy of Engineering
NRC	National Research Council [Canada]
NSN	National Supply Number
OER	oxygen evolution reaction
OMB	Office of Management and Budget
PEM	Proton Exchange Membrane
PVC	polyvinyl chloride
RDE	rotating disk electrode
RDS	rate determining step
SAR	same as report
SDS	sodium dodecyl sulfate
SEM	scanning electron microscope
TR	Technical Report
UCEAO	The University Clean Energy Alliance of Ohio
URL	Universal Resource Locator
US	United States
XRD	X-ray diffraction

References and Publications

References

Alexandrova, A. N., and W. L. Jorgensen. 2007. Why urea eliminates ammonia rather than hydrolyzes in aqueous solution. Journal of Physical Chemistry B 111(4):720-730.

Barrios, A. M., and S. J. Lippard. 2000. Interaction of urea with a hydroxide-bridged dinuclear nickel center: An alternative model for the mechanism of urease. Journal of the American Chemical Society 122(38):9172-9177.

Becke, A. D. 1993. A new mixing of Hartree–Fock and local density-functional theories. Journal of Chemical Physics. 98:1372. doi:10.1063/1.464304.

Benini, S., W. R. Rypniewski, K. S. Wilson, S. Miletti, S. Ciurli and S. Mangani. 1999. A new proposal for urease mechanism based on the crystal structures of the native and inhibited enzyme from Bacillus pasteurii: Why urea hydrolysis costs two nickels. Structure 7(2):205-216.

Boggs, B. K., and G. G. Botte. 2009. On-board hydrogen storage and production: An application of ammonia electrolysis. Journal of Power Sources. 192(2):573-581.

Boggs, B. K., R. L. King, and G. G. Botte. 2009. Urea electrolysis: Direct hydrogen production from urine. Chemical Communications, pp 4859-4861.

Cooper, M., and G. G. Botte. 2006. Hydrogen production from the electro-oxidation of ammonia catalyzed by platinum and rhodium on raney nickel substrate. Journal of the Electrochemical Society, 153(10):A1894-A1901.

Daramola, D. A., D. Singh, and G. G. Botte. 2010. Dissociation rates of urea in the presence of NiOOH catalyst: A DFT analysis. Journal of Physical Chemistry A. 114(43):11513-11521.

de Vooys, A. C. A., M. T. M. Koper, R. A. van Santen, and J. A. R. van Veen. 2001. The role of adsorbates in the electrochemical oxidation of ammonia on noble and transition metal electrodes. Journal of Electroanalytical Chemistry. 506(2):127-137.

Estiu G., and K. M. Merz. 2007. Competitive hydrolytic and elimination mechanisms in the urease catalyzed decomposition of urea. Journal of Physical Chemistry B. 111(34):10263-10274, http://pubs.acs.org/doi/abs/10.1021/jp072323o

Estiu, G., and K. M. Merz. 2004a. Enzymatic catalysis of urea decomposition: Elimination or hydrolysis? Journal of the American Chemical Society. 126(38):11832-11842. doi:10.1021/ja047934y, http://pubs.acs.org/servlet/linkout?suffix=ref3/cit3&dbid=20&doi=10.1021%2Fjp105159t&key=10.1021%2Fja047934y

Estiu, G., and K. M. Merz. 2004b. The hydrolysis of urea and the proficiency of urease. Journal of the American Chemical Society. 126(22):6932-6300. doi:10.1021/ja049327g, http://pubs.acs.org/servlet/linkout?suffix=ref4/cit4&dbid=20&doi=10.1021%2Fjp105159t&key=10.1021%2Fja049327g

Estiu, G., D. Suarez, and K. M. Merz. 2006. Quantum mechanical and molecular dynamics simulations of ureases and Zn β-lactamases. Journal of Computational Chemistry. 27(12):1240-1262.

Fearon, W. R. 1926. The biochemistry of urea. Physiological Reviews. 6(3):399-439.

Gaussian Inc. 2003. Gaussian 03 (software), http://www.gaussian.com/

Gerischer, H., and A. Mauerer. 1970. Untersuchungen zur anodischen oxidation von ammoniak an platin-elektroden. Journal of Electroanalytical Chemistry. 25(3):421-433.

Hay, P. J., and W. R. Wadt. 1985. Ab initio effective core potentials for molecular calculations. Potentials for the transition metal atoms Sc to Hg. Journal of Chemical Physics. 82(1):270. doi:10.1063/1.448799.

Hay, P. J., and W. R. Wadt. 1985b. Ab initio effective core potentials for molecular calculations. Potentials for K to Au including the outermost core orbitals. Journal of Chemical Physics. 82(1):299. doi:10.1063/1.448975.

Hehre, W. J., L. Radom, P. V. R. Schlayer, and J. A. Pople. 1986. Ab Initio Molecular Orbital Theory. New York: John Wiley & Sons.

M. B. Biradar. 2007. Design, scale-up, and intergration of an ammonia electrolytic cell with a proton exchange membrane (PEM) fuel cell. Chemical and Biomolecular Engineering. Athens,OH: Ohio University.

Marquez, Andres I., Frederic Vitse, and Gerardine G. Botte. 2004. Theoretical investigation of the electro-oxidation of ammonia. Electrode Processes VII, 206th Meeting of The Electrochemical Society, p 203, http://electrochem.org/dl/ma/206/pdfs/2000.pdf

Musiani, F., E. Arnofi, R. Casadio, and S. Ciurli. 2001. Structure-based computational study of the catalytic and inhibition mechanisms of urease. Journal of Biological Inorganic Chemistry. 6(3):300-314.

National Research Council (NRC) and National Academy of Engineering (NAE). 2004. The hydrogen economy: Opportunities, costs, barriers, and R&D needs. Washington, DC: The National Academies Press.

Oswin, H. G., and M. Salomon. 1963. The anodic oxidation of ammonia at platinum black electrodes in aqueous KOH electrolyte. Canadian Journal of Chemistry. 41(7):1686-1694.

Pickett, D. F., and J. T. Maloy, 1978. Microelectrode studies of electrochemically coprecipitated cobalt hydroxide in nickel hydroxide electrodes. Journal of the Electrochemical Society. 125(7):1026-1032, http://scitation.aip.org/getabs/servlet/GetabsServlet?prog=normal&id=JESOAN000125000007001026000001&idtype=cvips&gifs=yes&ref=no

Santen, R. A., and J. W. Niemantsverdriet. 1995. Chemical kinetics and catalysis. New York: Plenum Press.

SBW Consulting, Inc. 2002. Energy benchmarking secondary wastewater treatment and ultraviolet disinfection processes at various municipal wastewater treatment facilities. San Francisco, CA: Pacific Gas and Electric Company, http://www.cee1.org/ind/mot-sys/ww/pge2.pdf

Simka, W., J. Piotrowski, and G. Nawrat. 2007. Influence of anode material on electrochemical decomposition of urea. Electrochimica Acta. 52(18):5696-5703.

Vidotti, M., M. R. Silva, R. P. Salvador, S. I. C. de Torresi, and L. H. Dall'Antonia. 2008. Electrocatalytic oxidation of urea by nanostructured nickel/cobalt hydroxide electrodes. Electrochimica Acta. 53(11):4030-4034. doi:10.1016/j.electacta.2007.11.029, http://www.sciencedirect.com/science/article/pii/S0013468607013941

Simka, W., J. Piotrowski, A. Robak, and G. Nawrat. 2009. Electrochemical treatment of aqueous solutions containing urea. Journal of Applied Electrochemistry. 39(7):1137-1143.

Wadt, W. R., and P. J. Hay. 1985a. Ab initio effective core potentials for molecular calculations. Potentials for main group elements Na to Bi. Journal of Chemical Physics. 82:284. doi:10.1063/1.448800.

Wang, Dan, Wei Yan, and Gerardine G. Botte. 2011. Exfoliated nickel hydroxide nanosheets for urea electrolysis. Electrochemistry Communications. 13(10):1135-1138. doi:10.1016/j.elecom.2011.07.016.

Publications

The following sections lists technology transfer activities (posters, conference lectures, and journal publications) derived from this research.

Fourth Annual UCEAO (The University Clean Energy Alliance of Ohio) conference at Columbus, Ohio (April 20-21, 2010)

Hydrogen combustion applied to domestic water heaters (Poster)

Improvement of AgO cathode for Primary batteries (Poster)

Electro-oxidation of urea using rotating disk electrode (RDE) (Poster)

Theoretical study of the kinetics of ammonia oxidation on Pt(111) anodes (Poster)

Cathode optimization for hydrogen production through ammonia electrolysis (Poster)

217th The Electrochemical Society Meeting at Vancouver, Canada (April 25-30, 2010)

Theoretical investigation of ammonia oxidation kinetics on Pt(111) (Poster)

218th The Electrochemical Society Meeting at Las Vegas, Nevada (October 10-15, 2010)

Electric field effects on the adsorption of NH_3 on Platinum for electrochemical oxidation (Poster)

Electrochemical remediation of swine wastewater (Poster)

Identifying and adapting a solid polymer electrolyte for ammonia electrolysis (Talk)

Electro-oxidation of urea on NiOOH electrode (Talk)

In-situ Raman spectroscopic study of ammonia electro-oxidation in alkaline media (Talk)

Ammonia oxidation on platinum anodes: a DFT study of two mechanisms (Talk)

1st Advisory board meeting of the Center for Electrochemical Engineering Research (CEER), Ohio University at Athens, Ohio (November 11, 2010)

Electric field effects on NH_3 adsorption on Pt(111) electrodes (Poster)

In-situ Raman spectroscopic study of ammonia electro-oxidation in alkaline media (Poster)

Economic feasibility for residential power production using ammonia electrolytic cell (AEC) (Poster)

Evaluation of catalyst support materials for ammonia electrolysis (Poster)

Electrochemical remediation of swine wastewater (Poster)

Electro-oxidation of urea on NiOOH electrode (Poster)

Preparation and characterization of Ni/Co(OH)2 electrodes for the electro-oxidation of urea in alkaline solution (Poster)

Chemical conversion of urea to ammonia (Poster)

219th The Electrochemical Society Meeting at Montreal, Canada (May 1-6, 2011)

Evaluation of catalyst support materials for ammonia electrolysis (Talk)

Electrodeposition of rhodium on nickel electrodes for urea oxidation (Talk)

Denitrification of wastewater through ammonia electrolysis (Talk)

Journal publicationsg

Daramola, Damilola A., Deepika Singh, and Gerardine G. Botte. 2010. Dissociation rates of urea in the presence of NiOOH catalyst: A DFT analysis. Journal of Physical Chemistry A. 114(43):11513-11521.

King, Rebecca L., and Gerardine G. Botte. 2011. Hydrogen production via urea electrolysis using a gel electrolyte. Journal of Power Sources. 196(5): 2773-2778.

King, Rebecca L., and Gerardine G. Botte. 2011. Investigation of multi-metal catalysts for stable hydrogen production via urea electrolysis. Journal of Power Sources. 196(22):9578-9584.

Wang, Dan, Wei Yan, and Gerardine G. Botte. 2011. Exfoliated nickel hydroxide nanosheets for urea electrolysis. Electrochemistry Communications. 13(10):1136-1138.

REPORT DOCUMENTATION PAGE

1. REPORT DATE (DD-MM-YYYY)	2. REPORT TYPE	3. DATES COVERED (From - To)
26-01-2012	Final	

4. TITLE AND SUBTITLE	5a. CONTRACT NUMBER
Electro Decomposition of Ammonia into Hydrogen for Fuel Cell Use: Phase-I Study	5b. GRANT NUMBER
	5c. PROGRAM ELEMENT

6. AUTHOR(S)	5d. PROJECT NUMBER
Gerardine G. Botte and Carl A. Feickert	MIPR
	5e. TASK NUMBER
	5f. WORK UNIT NUMBER
	W917PM10612813

7. PERFORMING ORGANIZATION NAME(S) AND ADDRESS(ES)	8. PERFORMING ORGANIZATION REPORT NUMBER
U.S. Army Engineer Research and Development Center (ERDC) Construction Engineering Research Laboratory (CERL) PO Box 9005, Champaign, IL 61826-9005	ERDC/CERL TR-12-1

9. SPONSORING/MONITORING AGENCY NAME(S) AND ADDRESS(ES)	10. SPONSOR/MONITOR'S ACRONYM(S)
Director, Command, Control, Communications Systems HQDA, Deputy Assistant Secretary of the Army for Research and Technology 2800 Crystal Drive, 5th Floor, Suite 513 Arlington, VA 22202	11. SPONSOR/MONITOR'S REPORT NUMBER(S)

12. DISTRIBUTION/AVAILABILITY STATEMENT
Approved for public release; distribution is unlimited.

13. SUPPLEMENTARY NOTES

14. ABSTRACT

This work was undertaken to create an efficient process for electrolyzing ammonia, by clarifying the electrolytic decomposition pathways of ammonia and urea. This project demonstrated the feasibility of using ammonia and urea electrolysis technologies to produce hydrogen as a potential fuel source for the fuel Proton Exchange Membrane (PEM) fuel cell back up power for training facilities and soldier camps, under the "Silent Camp" initiative. This was achieved with scaling of bench scale electrolyzer to a 50 W electrolyzer system known as the "GreenBox." The construction of the 50 W GreenBox depended on the development of the catalyst and fundamental understanding of the reaction mechanisms for ammonia and urea electrolysis. Significant progress in catalyst development was achieved by using chemical and electrochemical preparation techniques, and using the various state-of-the-art analytical methods funded through this project. A new synthesized material–nickel hydroxide nanosheets–has shown potential to be catalyst for urea electrolysis and catalyst support for ammonia electrolysis. The energy consumption for the ammonia electrolysis using the nickel based nanostructured electrodes is anticipated to be lower than 8.6 Wh per gram of hydrogen gas produced. The low energy consumption will provide a significant advantage when the GreenBox is combined with fuel cells.

15. SUBJECT TERMS
fuel cells, alternative energy, PEM

16. SECURITY CLASSIFICATION OF:			17. LIMITATION OF ABSTRACT	18. NUMBER OF PAGES	19a. NAME OF RESPONSIBLE PERSON
a. REPORT	b. ABSTRACT	c. THIS PAGE	SAR	66	19b. TELEPHONE NUMBER (include area code)
Unclassified	Unclassified	Unclassified			